THE EFFECT OF LANDUSE-LAND COVER CHANGES ON WATER BALANCE COMPONENTS USING QSWAT MODEL:
A CASE STUDY AT SHAYA WATERSHED, ETHIOPIA

M.Sc. THESIS

BAYU ATALE WEDAJO

HAWASSA UNIVERSITY, HAWASSA, ETHIOPIA

DECEMBER, 2020

THE EFFECT OF LANDUSE/LAND COVER CHANGES ON WATER BALANCE COMPONENTS USING QSWAT MODEL: A CASE STUDY AT SHAYA WATERSHED, ETHIOPIA

BAYU ATALE WEDAJO

A THESIS SUBMITTED TO DEPARTMENT OF WATER RESOURCES AND IRRIGATION ENGINEERING, SCHOOL OF GRADUATE STUDIES,

HAWASSA UNIVERSITY

IN PARTIAL FULFILLMENT OF THE REQUIREMENT FOR THE MASTER OF SCIENCE IN WATER RESOURCES ENGINEERING AND MANAGEMENT

DECEMBER, 2020

HAWASSA, ETHIOPIA

MSc. Thesis Advisors' Approval Sheet

This is to certify that the thesis entitled the effect of land-use/land cover changes on water balance components at Shaya Watershed in Genale-Dawa River Basin as MSc thesis. The thesis is submitted to department of Water Resource Engineering and Management by Bayu Atale under my supervision. Hence, I recommended that he has been fulfilled the requirement and hence he can submit the thesis to department.

Submitted by: Bayu Atale	____________ Signature	_________ Date
Major Advisor: Tewodros Assefa (PhD)	__________ Signature	_________ Date
Co_ Advisor: Teshale Tadesse (MSc)	____________ Signature	_________ Date
Approved by: _______________	____________ Signature	_________ Date

Examiners' Approval Sheet

We, the undersigned members of the Board of Examiners of the final MSc thesis defense by **Bayu Atale** have read his **MSc thesis** entitled the **effect of land-use/land cover changes on water balance components using QSWAT model: A case study at Shaya Watershed in Genale-Dawa River Basin, Ethiopia** and examined the candidate. This is, therefore, to certify that the MSc thesis has been accepted.

Tewodros Assefa (PhD)	____________	_________
Major Advisor	Signature	Date
Tekalegn Ayele (PhD)	____________	_________
External Examiner	Signature	Date
________________	____________	_________
Internal Examiner (1)	Signature	Date
________________	____________	_________
Internal Examiner (2)	Signature	Date
________________	____________	_________
SGS Approval	Signature	Date
________________	____________	_________
Department Head	Signature	Date

Declaration

I Bayu Atale declare that this thesis is my original work and has not been presented for a degree or other award in any other university and all sources of material that I used in this thesis have been duly acknowledged.

Bayu Atale

Email: bayuatale34@gmail.com

Signature: _________________

Acknowledgement

Above all, I would like to thank Almighty God for his mercy and grace upon me during all my works and in all my life. Next to God, I would like to express veneration to my parents MOM (Medanit Amenu) and DAD (Atale Wedajo) for their love, support and motivation in my life.

I would like to express gratitude for my employer, Madda Walabu University, for provision of the sponsorship.

I would like to express sincere appreciation to my advisor Dr. Tewodros Assefa, for his advice and valuable suggestions, encouragement and guidance from the inception to the completion of this research works. As well, he devoted his precious time to advise me suggested valuable comments in this study. His critical comment and strict guidance aided me to accomplish and realized this research work. I would like also to thank my co-advisor Mr. Teshale Tadesse for his support in this research works.

I would like to thank Ministry of Water, Irrigation and Electricity, National Metrological Agency, Geospatial and Information Institute of Ethiopia for their help by providing desirable data to conduct this thesis work.

The last but not the least, my special thanks goes to my sibling Yewubdar Atale and Natnael Atale for their appreciation, motivation and inspiration throughout this study.

With Best Regards

Bayu Atale

December, 2020

Table of Contents

Acknowledgement I
List of Abbreviation and Acronym V
List of Table VI
List of Figure VII
Abstract IX
1 INTRODUCTION 1
1.1 Background 1
1.2 Statement of the Problem 2
1.3 Objectives of the Study 4
1.3.1 General Objective 4
1.3.2 Specific Objective 4
1.4 Research Questions 4
1.5 Scope of the Study 4
1.6 Significance of the Study 5
2 LITERATURE REVIEW 6
2.1 Water Balance and Its Influencing Factors 6
2.2 Landuse/Land Cover classification 7
2.3 Remote Sensing 8
2.4 Landuse/Land Cover Change Effects on Water Balance Components 8
2.5 Landuse/Land Cover Change Impacts in Ethiopia 9
2.6 Hydrological Model 10
2.7 Hydrological Model Selection Criteria 11
2.8 QSWAT Model 12
2.9 Application of QSWAT Model 12
2.10 SWAT Calibration and Uncertainty Procedures (SWAT-CUP) 13
2.11 Simulation of Hydrologic Model 13
3 MATERIALS AND METHODS 15
3.1 Description of the Study Area 15
3.1.1 Location 15

3.1.2 Topographic Features ... 16
3.1.2 Hydro-Climatic Condition ... 16
3.1.3 Soil and Hydrogeologic Features ... 18
3.1.4 Drainage Density ... 19
3.2 Data Collection and Analyses ... 20
3.2.1 Landuse/Land Cover Change Analysis ... 20
3.2.1.1 Field Work ... 20
3.2.1.2 Satellite Image Processing ... 20
3.2.1.3 Landuse/Land Cover Classes ... 22
3.2.1.4 Supervised Classification ... 22
3.2.1.5 Accuracy Assessment ... 23
3.2.1.6 Landuse/Land Cover Change Detection ... 24
3.2.2 Landuse/Land Cover Changes Response to Water Balance Components ... 24
3.2.2.1 QSWAT Model Setup ... 25
3.2.2.2 Discharge and Precipitation Data ... 27
3.2.2.3 Potential Evapotranspiration ... 29
3.2.2.4 Double Mass Curve Method ... 30
3.2.2.5 Water Balance Estimation ... 31
3.2.2.6 Sensitivity Analysis ... 33
3.2.2.7 Model Calibration and Validation ... 33
3.2.2.8 Model Performance Evaluation ... 33
3.3 Research Flow Chart ... 35
4 RESULTS AND DISCUSSION ... 40
4.1 Landuse/Land cover Analysis ... 40
4.1.1 Landuse/Land cover Map ... 40
4.1.2 Quantification of landuse/land cover ... 42
4.1.3 Landuse/Land Cover Change Detection ... 43
4.2 QSWAT Model Output ... 47
4.2.1 Sensitivity Analysis ... 47
4.2.2 Model Calibration and Validation ... 49

4.2.3 Effect of LULCC on Water balance components.. 52
4.2.4 Water Balance Coefficient 58
4.2.5 Annual and Seasonal contribution of LULC changes to Water balances................ 59
5 SUMMARY AND CONCLUSION 62
5.1 Summary.. 62
5.2 Conclusion 63
REFERENCE... 65
ANNEX 72

List of Abbreviation and Acronym

CN	Curve Number
DEM	Digital Elevation Model
EGSII	Ethiopian Geospatial and Information Institute
GCP	Ground Control Point
GIS	Geographical Information System
GLUE	Generalized Likelihood Uncertainty Estimation
GPS	Global Positioning System
HRUs	Hydrological Response Units
LULC	Land-use/Land Cover
LULCC	Land-use/Land Cover Change
MCMC	Markov Chain Monte Carlo
MLC	Maximum Likelihood Classification
MOWIE	Ministry of Water, Irrigation and Electricity
NMA	National Metrological Agency
NSE	Nash-Sutcliffe Efficiency
Parasol	Parameter Solution
PBIAS	Percentage of Bias
PET	Potential Evapotranspiration
PPU	Percent of Prediction Uncertainty
SCS	Soil Conservation Service
SUFI2	Sequential Uncertainty Fitting
QSWAT	Quantum Soil and Water Assessment Tools
WBCs	Water Balance Components
WGEN	Weather Generator Model
USGS	United States Geological Survey

List of Table

Table 3.1 Hydrogeologic characteristics of Shaya Watershed 18

Table 3.2 Satellite image data 21

Table 3.3 Overview of LULC classes at Shaya watershed in the past time 22

Table 3.4 Input data of QSWAT model 25

Table 3.5 Areal coverage of Precipitation in Shaya Watershed 28

Table 3.6 Summary of annual mean areal precipitation in Shaya Watershed 29

Table 3.8 Soil and Landuse code were used in QSWAT model to simulate water balances ... 32

Table 3.9 Model Performance Criteria 34

Table 4.1 Summary of areal coverage in percentage of landuse/land cover classes…………..…42

Table 4.2 Dominant LULC classes altered ‘‘from-to’’ information for diverse land scenarios46

Table 4.4 Summary of most important sensitive parameter of Shaya Watershed 47

Table 4.5 Description and application of Selected Parameter 48

Table 4.6 Monthly streamflow calibration and validation for LULC map 2002 50

Table 4.7 Percentage of water balance coefficient in Shaya Watershed under four land scenarios 58

List of Figure

Figure 2.1 Water balance components. 6

Figure 3.1 Shaya Watershed……………………………………………………………...15

Figure 3.2 Topography and Slope Map of Shaya Watershed 16

Figure 3.3 Relationship between Inter variation of mean precipitation (1989-2018), potential evapotranspiration (1989-2018) and observed stream flow (1989-2014) in the watershed 17

Figure 3.4 Intra variation of a), b), c) areal temperature, precipitation and observed flow 17

Figure 3.5 Soil map and Hydrogeological features of Shaya Watershed 18

Figure 3.6 Drainage Density of Shaya Watershed 19

Figure 3.7 Theissen Polygon Method 28

Figure 3.8 Potential evapotranspiration at sub-watershed scale for 1989 land map 30

Figure 3.9 Double mass curve analysis (1989-2018) 31

Figure 3.11 The QSWAT Model Structure 32

Figure 3.12 General frame work formats in the study area 35

Figure 4.1 Dominant LULC Classes in Shaya Watershed for land scenarios 1989, 2002, 2011 &2019………………………………………………………………………………..……41

Figure 4.2 Summary of areal coverage in percentage of landuse/land cover classes 42

Figure 4.3 Dominant LULC classes altered ‘‘from-to’’ information for diverse land scenarios 44

Figure 4.4 Monthly observed and simulated flow for long-term period (1991-2014) 49

Figure 4.5 Calibration and Validation of observed hydrograph for land map 2002 51

Figure 4.6 Scatter plot of observed and simulated flow at monthly scale 51

Figure 4.7 Water balance components at sub-watershed level under land scienarios a,b,c,d for 1989,2002,2011 &2019 respectively. 57

Figure 4.8 a) simulated runoff coefficient and ratio of evapotranspiration to precipitation (ET/P) and b) change of surface runoff to streamflow (Qs/Q), baseflow to streamflow (Qb/Q) and lateral flow to streamflow (Ql/Q) in long term period (1989-2019) in Shaya Watershed.................. 59

Figure 4.9 Changes of mean annual and seasonal contribution of surface runoff (SURQ), groundwater flow (QW_Q) and lateral flow (LAT_Q) as a),b),c) and evapotranspiration (ET), total streamflow (Q) as d),e),f) for baseline-altered period of (1989-2002,1989-2011,1989-2019)respectively. 61

Abstract

Ethiopia has experienced considerable land-use/land cover changes which altered the hydrological processes in many watersheds due to expansion of agriculture and population growth. This change can affect the water quality and quantity in space and time; thus, contribute to the deterioration of living conditions. Therefore, to address this concern, the semi-distributed model must able to reveal the effect of land-use/land cover changes on water resources for integrated watershed management. In this study, the change in land-use/land cover at Shaya Watershed in Genale-Dawa River Basin were evaluated by ERDAS IMAGINE software and using satellite image data (Landsat 5TM,7ETM,8OLI) for the proposed four land classification (1989,2002,2011,2019). The dominant classes were classified such as agriculture, forest, shrubland, grassland, bareland and settlement. The overall kappa statistics of land-use/land cover classification for each of the land map were found to be in the range of acceptance criteria based on literature (i.e. $\geq$ 0.8). The result revealed that forest, grassland, bareland and shrubland coverage decreased from (38.47% to 27.84%), (18.8% to 8.92%), (3.26% to 1.12%) and (16.55% to 15.53%) between (1989-2019) period respectively. Whereas, agriculture and settlement coverage increased from (20.41% to 38.38%) and (2.54% to 8.25%) in the same period. The QSWAT model has been used to estimate water balance components under land-use/land cover phases. The calibrated and validated of this model performance were evaluated based on R^2, NSE and PBAIS values which indicated good agreement between observed and simulated discharge. The effect of land-use/land cover changes were assessed by four land scenarios in which climate data (1989-2018), soil map and slope map were kept same, and only the land-use map were changed. The result showed that land-use/land cover have resulted in corresponding increase in surface runoff to streamflow, and decrease in base flow to streamflow and lateral flow to streamflow. Surface runoff to streamflow has increased from (26.4% to 30.7%), and base flow to streamflow has decreased from (65% to 61.1%) in the period of (1989-2019). But, slightly decreased were seen in lateral flow to streamflow from (8.7% to 8.2%) in the same period. In addition, surface runoff increased by (14% & 2.8%) in rainy season(kiremt) and dry season(bega) while groundwater flow decreased by (11% & 6.3%) in the same season. The total flow increased by (1.6%) in kiremt and decreased by (3.9%) in bega; whereas ET increased by (0.4% & 0.8%) in kiremt and bega season. The change in water balances had been observed in past 30 years due to the factor of land-use/land cover changes in the watershed. The output of this study could be used for soil and water conservation in Shaya Watershed.

Keyword: Land-use/Land cover change, Shaya Watershed, QSWAT model, Water balance components

1 INTRODUCTION

1.1 Background

World Bank Group (2015) recognized that shifting from rural to urban societies would be predicting an enormous impact on economic, social, political, and environmental landscape in countries across the globe. As a result, population growth and shifting from rural to urban societies are drivers in land use and land cover changes. Thus, such drivers affect the water quality, quantity in space and time. So, land-use/land cover planning and management are needful for sustainability of water resources.

Land cover is the biophysical state of the earth's surface, includes distribution of vegetation, water, soil, and others physical features of land while land-use is the way in which land has been used by humans and their habitat, usually emphasis on the functional role of land as economic activities (Yadav et al., 2019). LULC change is a major issue concern with regards to changes in the global environment. Hence, Land-use/land cover change has a unique signature on the landscape and soil distribution, which giving rise to fluctuation of water balance components (Li *et al.*, 2019; Tesfalem and Behailu, 2018).

Hydrological components could be altered by human activities in which allocating fresh water for irrigation, industry, domestic water supply consumption (Majid, 2016). The limiting amount of fresh water on the earth's surface could be distributed in different sectors which leads to change the water balance components (Example: precipitation, surface runoff, stream flow, ground water recharge).

LULC change may have numerous impacts on watershed hydrology (Palmate et al., 2018). The impacts can be either positive or negative (example: deforestation causes increasing surface runoff, decreasing the rate of evapotranspiration (Marhaento et al., 2017) and afforestation is caused in opposite side of deforestation (Tesfahun and Dereje, 2019). On another hand, the impact of LULC expected to alter regional hydrologic conditions and results in variation of effects on water balance components in the world (Li et al., 2019). Furthermore, LULC has been changed especially in the developing countries those have agriculturally based in economic development and rapidly increasing population (Abbas et al., 2010).

Similarly, Ethiopia is one of the developing countries in north east Africa's, in which economic development depends on agricultural production and rapid population raise can cause serious problem in LULC changes. (Example: Ayele *et al.*, 2018; Tegegne et al., 2013) confirmed that LULC changes altered hydrological processes in most watersheds. This LULC change has the most crucial impact on both ground and surface water resources since it significantly alters the magnitude of river flows. It is a primary concern in watershed management as the land cover change can lead to increased flooding, soil degradation and decreased recharge (Tesfahun and Dereje, 2019; Gashaw *et al.*, 2018).

The most severe indicator of the LULC change impact in Ethiopia was the loss of water stored in the Lake Alemaya and its wetland system (Shimelis et al., 2009). Reduced river flow is also described by (Kassa & Forech, 2009) in Hare River in Southern Ethiopia which resulted in unsatisfied irrigation demand. In addition to this, LULC change has negative impact on the hydropower generation (Welde and Gebremariam, 2017), water supply (Tessema, 2011) sectors by decreasing reservoir inflow and storage capacity as a reason of sedimentation. However, in the context of Shaya Watershed, soil erosion, flooding and decreasing soil fertility results in decline of agricultural production, overgrazing leads in decreasing recharge and infiltration process were happened in latest time due to changes in LULC (Tesfahun and Dereje, 2019; Kassahun and Mohamed, 2018). Therefore, studying LULCC with respect to WBCs is a crucial option for preserving watershed.

1.2 Statement of the Problem

Shaya Watershed is found in the southeastern part of Genale-Dawa River Basin near Bale Mountains in Ethiopia. In this watershed, commonly agricultural practice and livestock breeding are the backbone of economic development for local communities. Some part of Bale Mountains National Park (BMNP) was found in this watershed, which plays economic development for local, regional and national level. Because of the endemic animal like Red Fox, Mountain Nyala and others were found in this park, and they have been visited by internal and external tourist that brought income of the region wisely. Since integrated watershed management and conservation are great issue in this watershed.

Recently, rapid population growth raises serious problems to LULCC in Ethiopia. The same is true in case of Shaya Watershed. The increment of population growth every year is causes increased in land demand, particularly, the need for production, housing, agriculture and water demand for domestic uses. Hence, People tend to ignore land-use capability and suitability which causes land degradation, soil erosion, flooding and distresses water balances (Nugroho et al., 2013). The LULC can directly affects the amount of evaporation, groundwater infiltration and overland flow that occurs during and after precipitation events. This factors, control the water yield of rivers and groundwater aquifer which are important for ecosystem function and human use (Marhaento, 2018; Owuor et al., 2016). Therefore, to address these concerns, understanding the effect of land-use/land cover changes on water balance components using hydrological model can enable to develop systematic plan for watershed management (Lyu et al., 2019; Gashaw et al., 2018; Naschen et al., 2019).

Hydrological models are essential approaches to assist and providing information about the management of land and water resources. Most of the comprehensive models were used to estimate WBCs under various environmental condition such as MIKESHE, HEC-HMS, WETSPA, QSWAT and SWAT (Premanand *et al.*, 2018; Devia et al., 2015; Neitsch *et al.*, 2011). MIKESHE model is not available free (Fang et al., 2018). The HEC-HMS model has limitations to simulate for HRUs due to sub-watershed was fixed by the interest of the user (Fang et al., 2018). WETSPA requires more spatial data for larger watersheds, and it is not applicable in the absence of quality of data, especially, in developing countries (Aish, 2014). SWAT model has been extensively used by researchers in various countries to simulate the WBCs in terms of LULC and climate changes (Getachew, 2013; Arnold, 2015; Gashaw *et al.*, 2018). Practically this model was applicable and more used in developing countries to simulate hydrological components (Arnold, 2015). Hence, semi-distributed model was applied to simulate WBCs in response to the LULCC in this study.

Generally, in this study area, the problem arises from LULCC due to human activities increases for need of daily food consumption, fuel, building houses, agricultural expansion to improve living conditions and economic developments. However, such activities have been applied without planning and misunderstanding of integrated watershed management. These actions are altering the WBCs that characterized in the watershed. Therefore, it needs control action and this is initiated to study the detailed analysis of LULCC on water balance components using QSWAT model for understanding the impact of this land use changes to adopt present and future water resource planning, designing, controlling and managing for sustainable ecosystem conservation.

1.3 Objectives of the Study

1.3.1 General Objective

The general objective of this study was to assess the effect of land-use/land cover changes on water balance components in Shaya Watershed by using the QSWAT hydrological model.

1.3.2 Specific Objective

The specific objective of the study was listed as below:

- To quantify the spatial and temporal variation of LULC changes over four periods in past using ERDAS IMAGINE (1989,2002, 2011, 2019).
- To compute and evaluate the impact of LULC changes to changes on WBCs in Shaya Watershed using modeling approach.

1.4 Research Questions

The main research question encompasses in this study to achieve the above-mentioned objectives were listed as follows:

- ✓ How to LULC shows the spatial and temporal changes over the past few periods?
- ✓ How will LULC change influence the water balances in the study area?

1.5 Scope of the Study

The aim of the study was mainly focused on assessment of the effect of LULC changes to water balance components in Shaya Watershed by using the selective QSWAT model. In this research, land-use/land cover classes were mapped, trend of proportion of each class of LULC was conducted, impact of LULC change response to water balances were examined. But, in this study climate, geology and other important variable are not included due to difficulty and complexity of investigating all hydrological events as together while time, budget and input data are the governing factors. Hence, the study was concerned on the change of LULC that affects some of the WBCs in the Shaya Watershed to adopt sustainability of the land and water resource management.

1.6 Significance of the Study

The main significance of the study was listed as below:

- ✓ Motivate and encourage the planner, policy maker and experts to formulate and implement effective, efficient the strategies to reduce the source of the impact of LULCC on water resources developments.
- ✓ Promoting watershed management program as local community-based participatory approaches for effective utilization of natural water resources.
- ✓ The output could further be used to decide on appropriate mitigation measures for effect of LULCC within or around the watershed.
- ✓ Admitting appropriate land and water conservation strategies for the future in the watershed with rational approaches to minimize the undesirable effect of LULC changes.
- ✓ The study supports to get a new perception of water resources challenges and creating an appropriate mechanism of sustainable watershed protection from the effect of LULC changes.

2 LITERATURE REVIEW

2.1 Water Balance and Its Influencing Factors

The term water balance is defined as the balance between input and output of water from precipitation and the outflow of water by evapotranspiration, groundwater recharge and streamflow or surface runoff. It is an efficient means for programming and evaluating in the scale of watersheds, applying for water supply and water allocation, waste water management and flood estimation (Anderson et al, 2006).

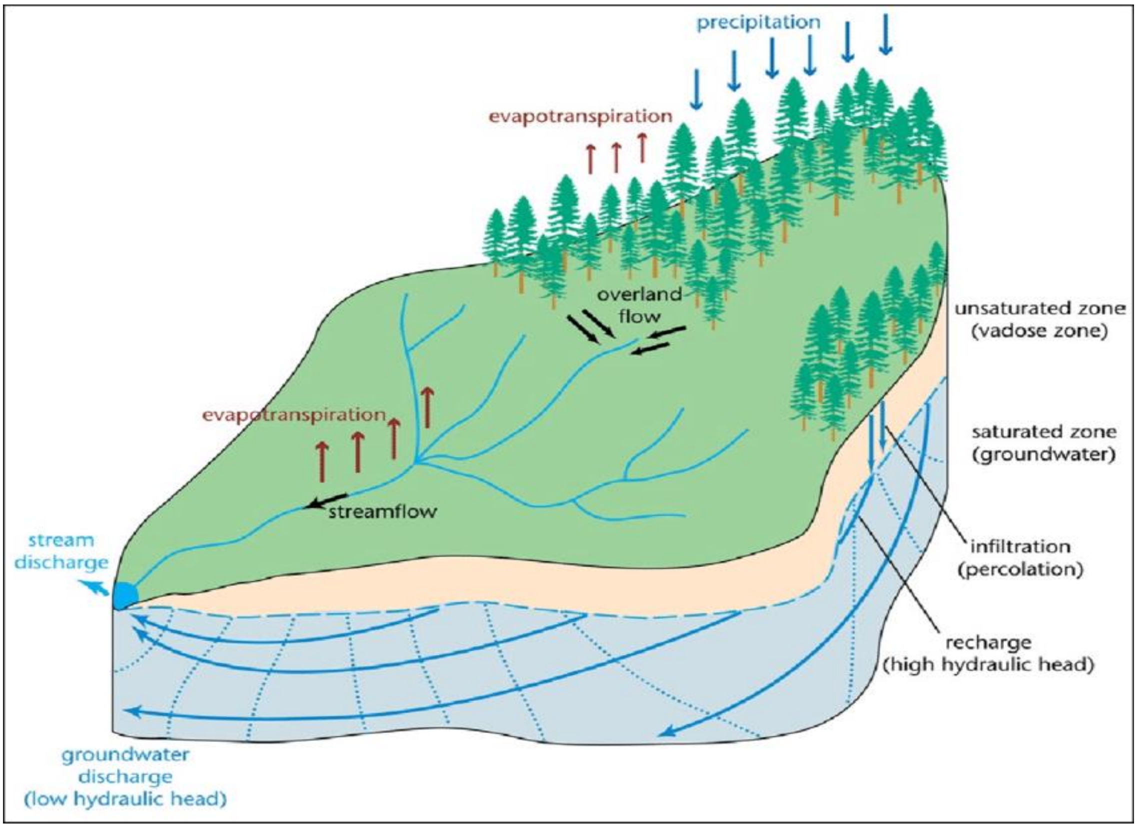

Figure 2.1 Water balance components (Smerdon et al., 2009)

Several factors affect WBCs in the watershed due to LULC changes in spatial and temporal series. These factor are population growth, urbanization, agricultural activities, deforestation and climate change and variabilities (Marhaento, 2018). Thus, such factors alter LULC that have greater consequences in social, economic, political, environmental and hydrological fluctuation in the watershed which leads to increase pressure on water demand and distribution.

2.2 Land-use/Land Cover classification

Thematic mapping from remotely sensed data is typically based on an image classification (Santillan et al., 2011). This can be analyzed by comparing different spectral reflectance. There are pixels and object-based classification of sensed images for various applications. In object-based models, geographical objects are considered as basic units for analysis instead of individual pixels (Kindu et al., 2013). In general, pixel-wise classification algorithms has two groups: unsupervised and supervised classification.

In unsupervised classification, the software is identifying statistical patterns of the image data without the help of any ground truth data. The image of pixels has been processed based on similar spectral characteristics. The advantage of this approach is involves the least user interaction which minimizes human error (Lillesand et al., 2008). But it is not always logical to merge points into meaningful land cover classes and not possible to improve the results by including expert knowledge about the study area into the process.

The supervised classification approach requires prior knowledge about land cover types that are to be classified and mapped (Santillan, 2011). The software used knowledge of the area and information collected during fieldwork as important inputs to classify the pixels into similar groups based on the training sample specified. Training sample selection depends on many factors that affect classification accuracy. According to Srinivasan and George (2015) noted that supervised classifiers produce better results when larger training sets are used. To achieve optimal outcomes, a balance between adequate training data and the accuracy requirements needs to be found (Getahun and Haj, 2015). Gumindoga et al. (2014) stated that the selection of sample training points is based on the relative proportion of each land cover type derived from visual interpretation of the image to ease of the survey, variety of features present, weather condition, and so on.

Various supervised classification systems might be used to assign an unknown pixel to one of many classes. The maximum likelihood classification (MLC) is one of the most common popular methods of supervised classification technique (Santillan et al., 2011). It is known for its ability to establish a good separation between classes and improving the accuracy of classification (Thakkar et al., 2015).

2.3 Remote Sensing

Remote sensing is particularly used to find out the response of the earth 's surface based on the features of the ground surface, including the natural or artificial land cover. According to Santillan et al. (2011), remote sensing can provide long term global hydrological variables, even for remote and inaccessible regions of the earth. It is a modern tool to detect and track land cover change at various scales.

The spatial resolution can determine the level of spatial detail on the earth's surface. A fine-scale high spatial resolution data such as IKONOS, Quick Bird, and SPOT 5 providing a greater potential to extract much more detailed information on land cover structures than medium or coarse spatial resolution data. Yet, data emerge, shadows caused by topography, tall buildings or trees, and the high spectral variation within the same land-cover classes are some related problems. At a regional scale, medium spatial resolution data such as Landsat TM/ETM+ and Terra ASTER are the most used data. At a continental or global scale, coarse spatial resolution data such as MODIS are preferable.

Besides, many researchers worked with various sensor data in monitoring LULC changes, among them, (Butt et al., 2015), who used Multispectral Landsat 5 and SPOT 5 in Simly Watershed, Pakistan, while Arafat et al. (2014) used SPOT4 (HRVIR) images with 20 m spatial resolution Mapping of North Sinai. Tesfahun and Dereje (2019) applied medium-resolution Thematic Mapper (TM) and Enhanced Thematic Mapper (ETM) in Weib Catchment of Ethiopia. Yesuf *et al.* (2015) also used SPOT 5 satellite image and ortho rectified photographic images in the Lake Hayq closed drainage basin. Hence, in this study, TM, ETM and OLI_TIRS had to detect LULC change impact on water balances to understand future watershed management.

2.4 Land-use/Land Cover Change Effects on Water Balance Components

According to Naschen et al. (2019) stated that LULC changes in which caused by the rise of urbanization, agricultural activities and deforestation are the cause factors for the changes of WBCs (surface runoff, evapotranspiration, groundwater recharge). So, urbanization has been caused to increases surface runoff and decreases evapotranspiration (Tesfalem and Behailu, 2018; Addae and Oppelt, 2019); agricultural expansion activities leads to soil erosion, vegetation cover reduced, etc. Deforestation could bring environmental climate changes with significantly minimizing local and regional precipitation accessibilities and rising flood frequency.

Various scholars used land cover mapping tools and methods to understand the LULC change impact on the hydrologic behavior of watersheds (e.g. Hamad et al., 2018; Yesuf *et al.*, 2015; Ayele *et al.*, 2018). In view of these, the effect of deforestation has reduced infiltration/base flow (Tesfahun and Dereje, 2019; Welde and Gebremariam, 2017) and increased in surface runoff (Tesfalem and Behailu 2018).

Changes in LULC could affect soil health (soil quality) or soil intactness (the ability of soils to stay in place) and increased the risk of erosion (Shiferaw, 2011). Consequently, it affects water supply, reservoir storage capacity, agricultural productivity and freshwater ecology by increasing sediment yield (Li et al., 2015). Owuor et al. (2016) indicated that restoration of bare land leads to changes in soil hydro-physical conditions (e.g. texture, hydraulic conductivity, bulk density, porosity, etc.) which in turn results in reduced low flows and groundwater recharge. Surface-water quality is also sensitive to LULC changes which results considerable impact on ecosystems, biotic systems, even on human health (Zamani et al., 2013; Bansode and Patil, 2016).

2.5 Land-use/Land Cover Change Impacts in Ethiopia

Many researchers so far have conducted in several parts of Ethiopia that reveals different results of LULC change impact with various approaches. For instance, Getahun and Haj (2015) studied the impact of LULC changes at Melka Kuntrie sub basin in which the result shows that a slightly higher streamflow under land cover changes. In the same way, stream flow of Gilgel Abbay Watershed has increased, whereas the ground water flow has decreased.

Another study by Jemberie and Gebremariam (2016) in Gilgel Abay catchment indicated that an increase of cultivation, decrease of grass and shrub land are produced loosening and erosion of a soil particle. Consequently, it caused an increase in sediment yield especially during peak flow periods. Rientjes *et al.* (2011) also evaluated the land cover change impact in the Upper Gilgel Abbay catchment of the Upper Blue Nile Basin. There is a significant decrease in forest cover mainly due to expansion of agricultural land. As a result, the annual and the peak flows of the catchment increased by 13% and 46% respectively while the low flows decreased by 35%.

The recent studies in the Beressa Watershed, Northern Central Highland of Ethiopia showed that forest cover and water body were increased as a result of the initiation of watershed management by local communities activities that taken to restore trees around their home and farm lands (Andualem and Gebremariam, 2016). An expanded of agricultural land and settlement as well as decrement of forest and grassland in Lake Ziway Catchment were leads to increase the mean monthly flow by 3.8% in wet and decreased flow by 12.3% in dry season (Tufa et al., 2015).

Another study by Setegn et al. (2009) in Lake Alemaya Eastern highlands of Ethiopia showed that the area adjacent to the lake are constantly cultivated which cause serious problem of soil erosion and increased the sedimentation at the lake. This is, therefore, the volume of water has been decreased over time. Welde and Gebremariam (2017) focused a similar study in Tekeze dam catchment. In such study, the outcome stated that bare land and agricultural land were increased mean annual stream flow by 6.02% and sediment yield amounts by 17.39%.

Moreover, Kassa and Forech (2009) assessed watershed hydrological responses to changes in LULC and management practices at Hare Watershed rift valley basin. The result of the analysis showed that expansion of crop land contributed to an increase in run-off and reduction on dry-season flows. Similarly, farmlands and settlements expansion in Hare Watershed mostly associated with the decrease in forest class.

Generally, the effect of land-use/land cover changes on water resources in Ethiopia is obviously known as mention in above among many selected watersheds. In this document, studying the effect of LULC changes on water balance components in Shaya Watershed is essential for decision-making process for multiple water resource developments like small-scale irrigation, water supply, soil erosion control and others.

2.6 Hydrological Model

Hydrological models are scientific descriptions of components of the hydrologic cycle. The model is in general designed to get a better understanding of the hydrologic processes in the watershed. The watershed hydrologic models could be developed for various purposes and therefore have numerous forms (Devia et al., 2015).

Hydrological models are categorized based on model input and parameters and the extent of physical principles applied in the model (Devia et al., 2015). There are many arrangements of hydrologic models, deterministic versus stochastic, lumped versus distributed and etc. On the basis of process, description, the hydrological models can be classified in to three main categories (Cunderlik, 2003).

a) Lumped models: Parameters of lumped hydrologic models do not vary spatially within the basin and thus, basin response is evaluated only at the outlet, without clearly accounting for the response of individual sub basins. The parameters often do not represent physical features of hydrologic processes and usually involve certain degree of observation.
b) Distributed models: Parameters of distributed models are fully allowed to vary in space at resolution chosen by the user. Distributed modeling approach attempts to incorporate data concerning the spatial distribution of parameters together with computational algorithms to evaluate the influence of this distribution on simulated precipitation runoff behavior. Distributed models generally require large amount of data.
c) Semi-distributed models: Parameters of semi-distributed models are partially allowed to vary in space by dividing the basin in to a number of smaller sub basins. The main advantage of these models is that their structure is more physically based than the structure of lumped models and need less input data than fully distributed models. QSWAT, HEC-HMS and HBV are considered as semi-distributed models.

2.7 Hydrological Model Selection Criteria

There are many criteria which can be used for choosing the right hydrologic model. The four fundamental criteria that must be considered for model selections are:

1. Identification of the objective
2. Skill has been needed about the model
3. Visualization of the model to be demonstrated to estimate the desired outputs adequately
4. Availability of input data

For this study QSWAT (semi-distributed model) is selected because its structure is more physically based than the structure of the lumped model, freely available, better visualize the result and meets the objective of the study.

2.8 QSWAT Model

QSWAT is a quantum soil and water assessment tool which is completely revised version of SWAT model and uses similar equation of SWAT to simulate hydrological processes. The only difference was the modification of code in the database and the internal structure updated with adjustment of time management and avoidance of error made as duplicating output of watershed information. As Arc SWAT is the interface of ArcGIS whereas QSWAT is the interface of QGIS. In this study, QGIS version 2.6.1 was used to interface of QSWAT model for water balance simulation (Dile et al., 2019).

Therefore, QSWAT model is a semi-distributed hydrologic model working on a daily time step and uses a modified soil conservation service-curve number (SCS-CN) method to calculate runoff (Premanand et al., 2018; Baker and Miller, 2013). It is developed for assessing the impact of management and climate on water supplies, sediment and agricultural chemical yields in watersheds and larger river basins. The major components of QSWAT include hydrology, weather, erosion, plant growth, nutrients, pesticides, land management and stream routing.

2.9 Application of QSWAT Model

QSWAT model has been applied in hydrological watersheds and successfully calibrated and validated in many areas of the world. The studies indicated that the SWAT model is capable of simulating the hydrologic process from complex and poor data in the watershed with reasonable model performance statistical values (Abbaspour et al., 2018). Premanand *et al.* (2018) were used QSWAT model for uncertainty analysis of stream flow simulation in patapur watershed. Kashinde and Patil (2017) were applied the QSWAT model to studied water balance of the watershed at Aurangabad District. Adeogun *et al.* (2014) was used SWAT models to predict water balance and water yield of a catchment area in Nigeria. It was suggested that SWAT model could be a promising tool to predict water balance and water yield in sustainable management of water resource.

Tegegne et al. (2013) was applied SWAT model on Lake Tana Reservoir Water Balance and reported that, the overall model performance was satisfactory. Similarly, (Tibebe and Bewket, 2011) also applied SWAT model to evaluate surface runoff generation and soil erosion rates for a small watershed (Keleta Watershed) in the Awash River Basin, Ethiopia, and recommended that, the SWAT model provides a useful tool for soil erosion assessment for watersheds and facilitates planning for a sustainable land management. Tufa et al. (2015) was applied SWAT model for assessing land use/land cover impacts on stream flow in Ketar watershed and recommended that, the SWAT model used for further future research. The above literature review indicated that the SWAT model could are capable of simulating the hydrological process with reasonable accuracy and can be applied to large and complex watersheds.

2.10 SWAT Calibration and Uncertainty Procedures (SWAT-CUP)

Distributed watershed models are increasingly being used to support decision making in land use change. These models should pass through a careful calibration and uncertainty analysis. Large scale distributed models are difficult to calibrate and to interpret the calibration because of large model uncertainty, input uncertainty and parameter non-uniqueness. However, SWAT-CUP is one of the programs which is currently used by different researchers. It is a public domain and any calibration, uncertainty or sensitivity can be linked to SWAT. The program links Generalized Likelihood Uncertainty Estimation (GLUE), Parameter Solution (ParaSol), Sequential Uncertainty Fitting (SUFI2) and Markov Chain Monte Carlo (MCMC) procedures to SWAT (Abbaspour et al., 2018). It enables sensitivity analysis, calibration, validation and uncertainty analysis of QSWAT models. In this study, SUFI2 method was used to determined uncertainty analysis of stream flow through the sequential and fitting process in which iteration and unknown parameter estimates are achieved before the final estimates.

2.11 Simulation of Hydrologic Model

The SWAT model was designed in the 1990s to predict the impact of land management practices such as LULC changes on water balance and spatial distribution of surface runoff in large complex watersheds over long periods of time (Neitsch et al., 2011). The model spatially predicts the impacts at the sub basin even at the Hydrologic Response Units (HRUs) level (Githui et al., 2009). Where HRUs represent the portion within the sub-basin that is comprised of a unique land cover, soil and slope combinations. HRUs is categorizing within the sub basins increases modeling accuracy and provides a better physical representation.

QSWAT requires spatial (soil, topography and land use) and temporal data (weather, hydrology) to set up and run the model (Dile et al., 2019). It is simulating the hydrological variables based on the water balance equation (Arnold, 2015) as shown in equation (1).

$$Sf = Si+(P-Qs-ET-Wseep-Qb) \text{ ………. (equation1)}$$

Where: Sf - final soil water content (mm), Si - initial soil water content, P - precipitation, Qs - surface runoff, ET - evapotranspiration, Wseep - amount of water entering the vadose zone from the soil profile and Qb - amount of return flow on day (mm). Runoff in this study could be estimated using the Soil Conservation Service (SCS) curve number (CN) method. This method showed better efficiency during computation and prediction of runoff depth with a given rainfall event (Tibebe and Bewket, 2011; Holder et al., 2019). CN was determined runoff yield based on land use types, soil group, and hydrologic conditions. The SCS-CN method computes runoff using equation (2).

$$Qs = \frac{(\mathrm{P} - 0.2S)^2}{\mathrm{P} + 0.8S} \text{ ……………. (equation2)}$$

Where Qs is the daily surface runoff (mm), P is daily rainfall depth (mm), and S is the retention parameter (mm). The retention parameter (S) in (mm/day) is determined based on equation (3) below.

$$S = \frac{25400}{CN} - 254 \text{ ………………. (equation3)}$$

3 MATERIALS AND METHODS

3.1 Description of the Study Area

3.1.1 Location

Shaya Watershed is found in southeastern part of Ethiopia in Oromia Regional State, Bale Zone. As shown in figure 3.1 below, this watershed is located in Genale-Dawa River Basin at upper parts of Weib sub-basin and its geographic coordinates is bounded between 6°50' - 7°15' N latitudes and 39° 46' - 40° 00' E longitudes.

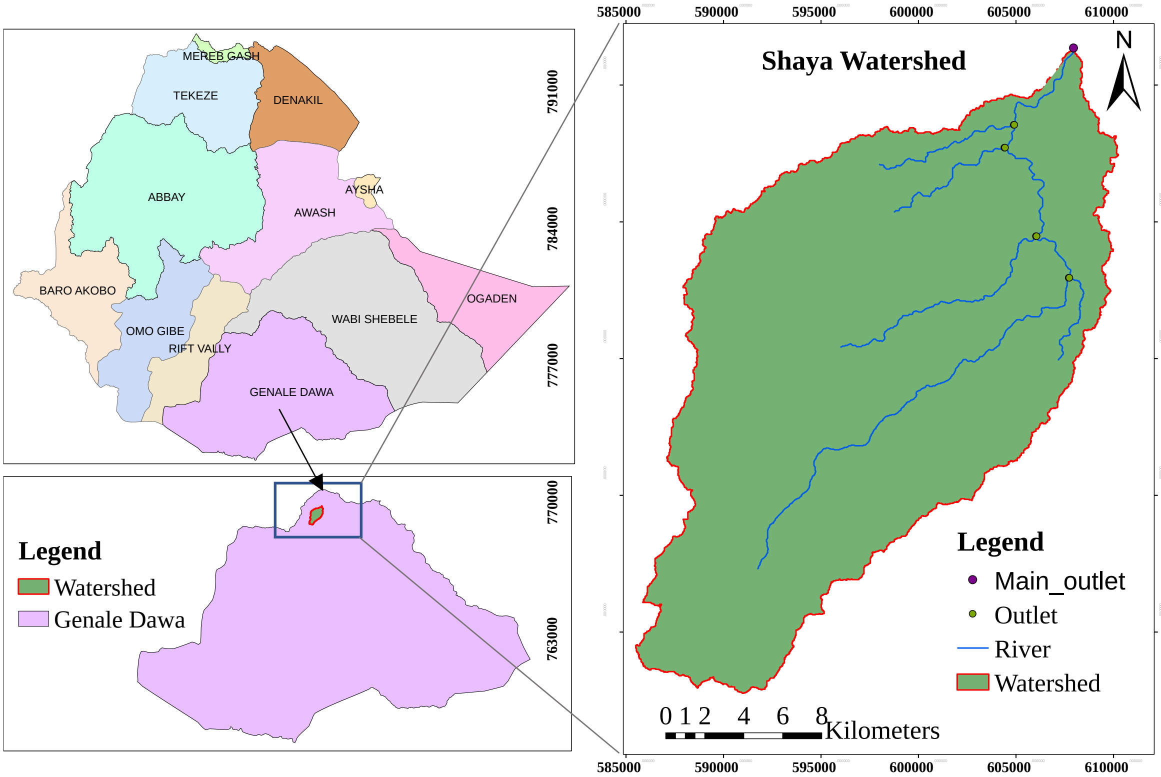

Figure 3.1 Shaya Watershed

In this watershed, the river is generated at northern borders of Bale Mountains and flows initially at north-east direction before joining with Weyb River. Then the river channel where drain to south-east wards on their own courses. Finally, the river flow can merge in Genale-Dawa River near the Ethio-Somalia border and has potential to reach up to Somali lowlands (Serur and Sarma, 2016). The entire watershed area is 453 km^2 and has multiple economic activities experienced with various environmental diversities.

3.1.2 Topographic Features

The figure 3.2 revealed that the digital elevation model (DEM) of Shaya Watershed. The watershed is originating from high altitude of 4,356m.a.s. l in the Bale Mountains and drains to low altitude of 2,398m.a.s. l at the outlet of the watershed.

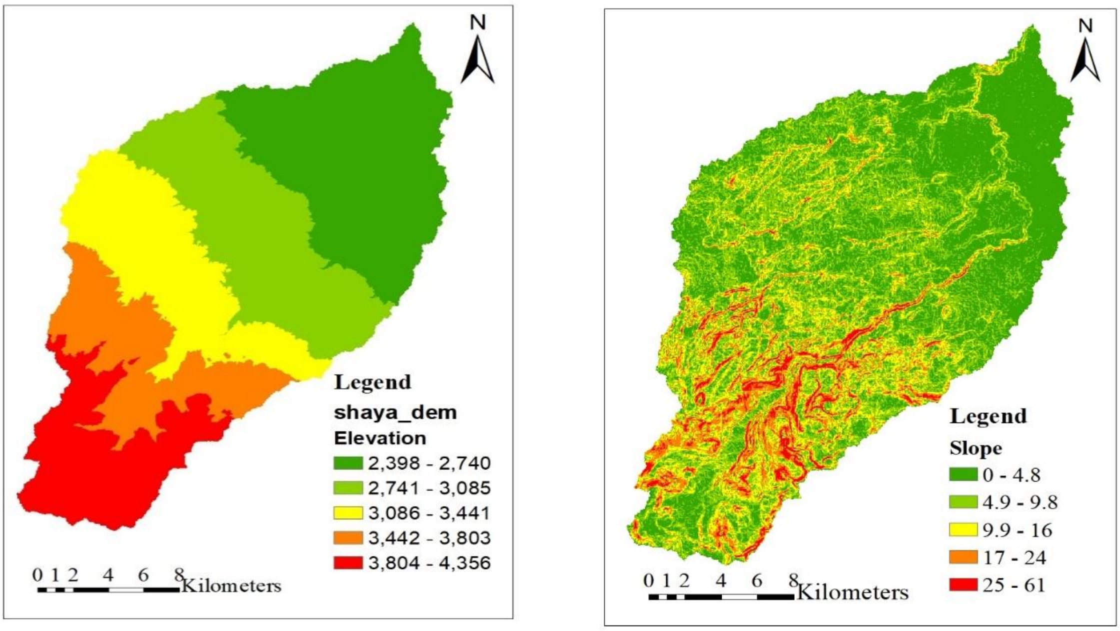

Figure 3.2 Topography and Slope Map of Shaya Watershed

Altitude decreases from south to north direction in the watershed as shown in figure 3.2. The upper part of watershed was the steepest while the middle and the downstream part were flat to the gentle slope respectively which is suitable for agricultural activity.

3.1.2 Hydro-Climatic Condition

The climate of Shaya Watershed is extended from range of frost (Wurch) at the uppermost part near Senate Mountain to humid highlands of Bale Mountains National Park (Serur & Sarma, 2016). The rainfall pattern in the study area is bimodal type that is main rainy season in Kiremt (June to October) and short rainy season Belg (March to May) (Kassahun and Mohamed, 2018). The distribution of rainfall in study area is uneven which is a source of the perennial river. The mean annual rainfall, potential evapotranspiration and stream flow in the watershed were ranges between 700-1800 mm, 650-950mm, and 150-750mm respectively (see figure3.3).

In addition, the average annual maximum and minimum temperature in the watershed are about 19.9 ℃ and 6.5℃ for 30 (1989-2018) years respectively.

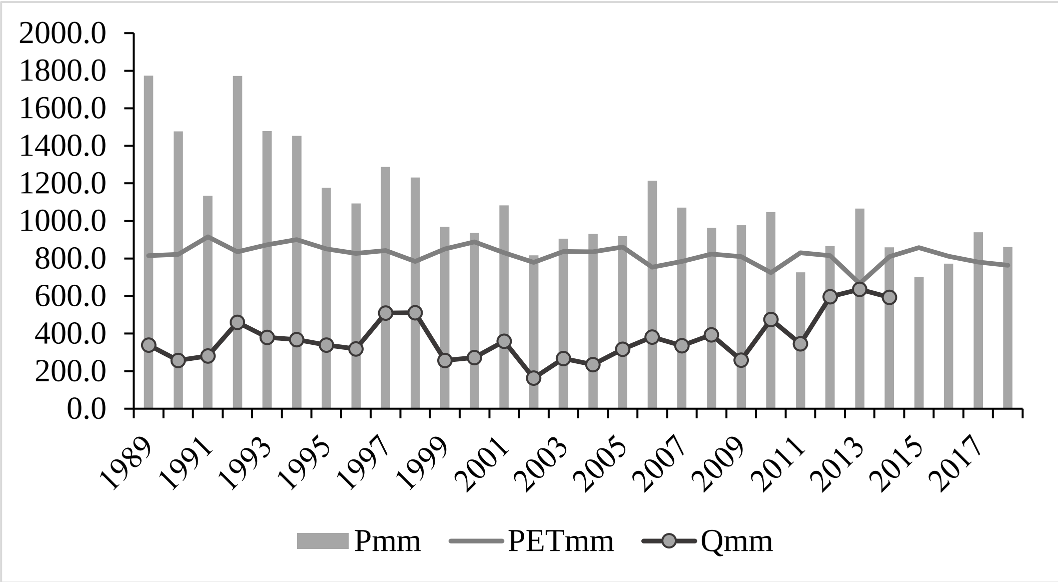

Figure 3.3 Relationship between Inter-annual variation of mean precipitation (1989-2018), potential evapotranspiration (1989-2018) and observed stream flow (1989-2014) in the watershed

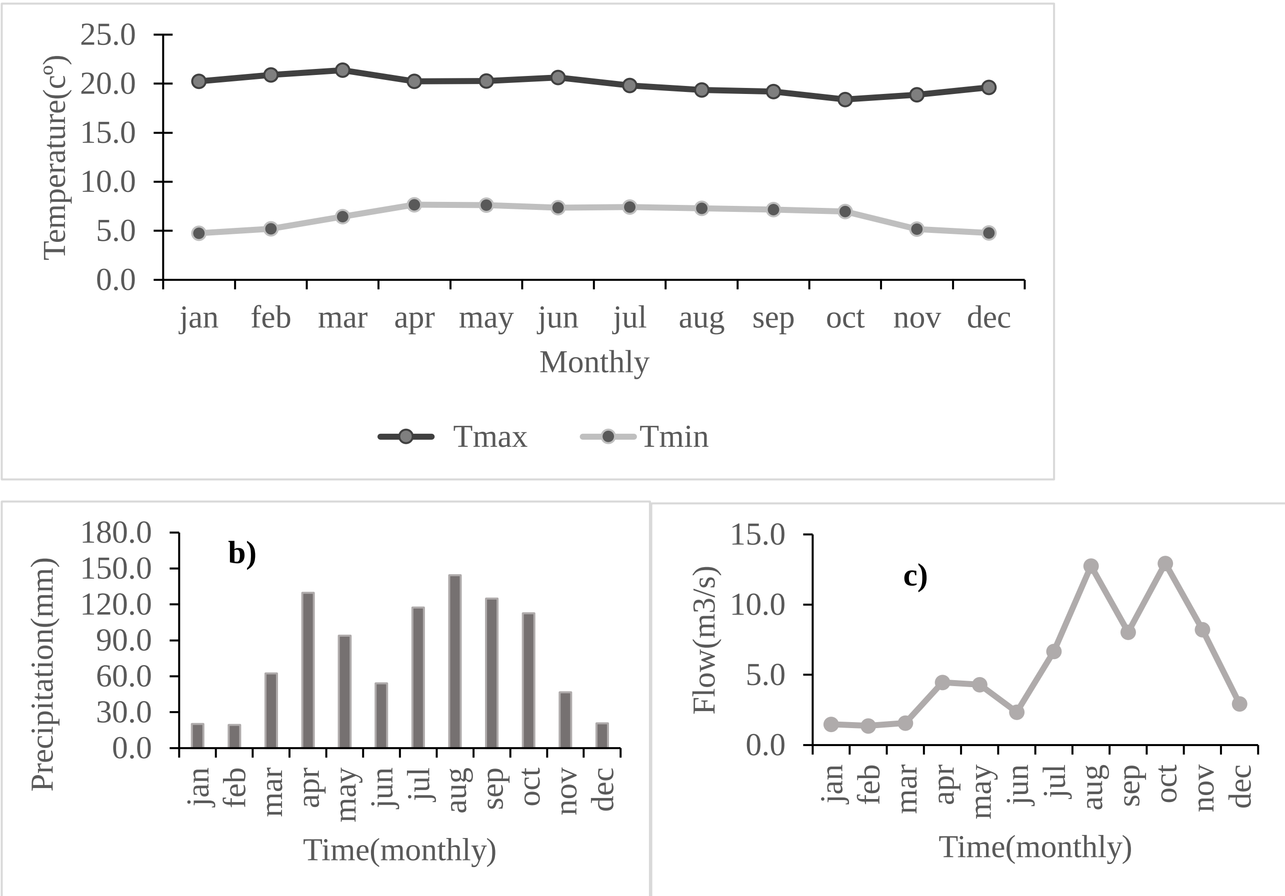

Figure 3.4 Intra variation of a), b), c) areal temperature, precipitation and observed flow

3.1.3 Soil and Hydrogeologic Features

Soil texture, structure, arrangement are leads to affect the soil moisture content, field capacity and bulk density for plant development in the watershed. Soil is crucial elements to determine water balance variables like runoff, ground water recharge, water contents. The soil groups found in the watershed are Cambisol, Luvisols and Regosol (MWIE, 2019). In figure 3.5 below indicated that Dystric- cambisoil and Regosol are found mostly in the upper edge of the watershed. Whereas, Eutric-cambisols and Chromic-Cambisols are found commonly in the middle of the watershed and Haplic-luvisol and Vertic-luvisol are found at the downstream of the watershed.

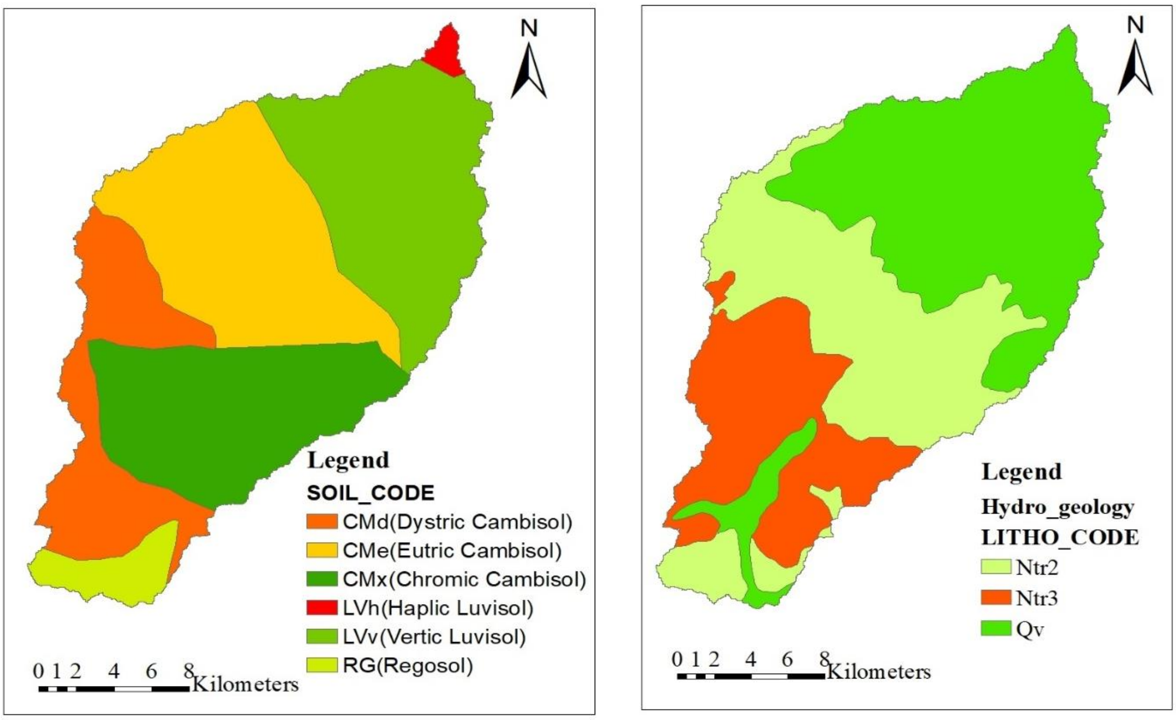

Figure 3.5 Soil map and Hydrogeological features of Shaya Watershed

The aquifer structures in the watershed were volcanic rock (MWIE, 2019). This volcanic rock can characterize as low, moderate and high permeability of water in the watershed.

Table 3.1 Hydrogeologic characteristics of Shaya Watershed

S. N	Symbol	Permeability	Description
1	Ntr2	moderate	Extensive aquifer with fracture permeability
2	Ntr3	low	Extensive aquifer with fracture permeability
3	Qv	High	Extensive aquifer with fracture permeability

From table 3.1, high to moderate permeability of water capacity were found in downstream parts; whereas the moderate and low permeability of water could be found in middle and the upstream zone of the watershed due to variation in altitude and land-use/land cover types.

3.1.4 Drainage Density

Drainage density is one of the watershed characteristics that defines as the total length of the channel(stream) over the whole area of the watershed. This density was derived from DEM of watershed by ArcGIS software as shown in figure3.6. It is difficult to determine drainage density of the watershed due to complexity of stream network in nature. But, approximately the lower and higher drainage density were found to be (0 - 3.4km/km^2) in the watershed.

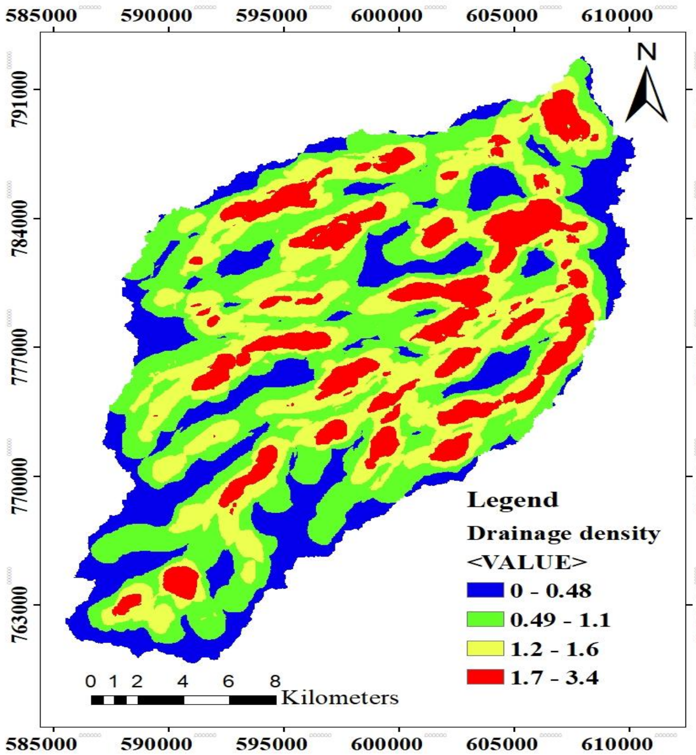

Figure 3.6 Drainage Density of Shaya Watershed

Figure 3.6 above indicated that the drainage density of study area; the red color implies high drainage density which shows high surface runoff rapidly takes place over the channel, as well as low infiltration rate and sparce vegetation cover (Yalcin, 2008) were found to be in this area. In the same way, the blue color reveal as low drainage density that characterized by low surface runoff and high recharge (Yalcin, 2008) at this watershed area. This drainage density also important to indicate the potential zone of groundwater availability (high recharge =high GW potential).

3.2 Data Collection and Analyses

3.2.1 Land-use/Land Cover Change Analysis

3.2.1.1 Field Work

To produce proper LULC classes in the study area, field observation is one of the key elements to show good validation of image classification with closely links to ground control points (GCP) for making image rectification and georeferencing. In this study, classification of LULC was applied by using satellite images and GIS-based techniques, ground control points (GCPs) which could be served to determine the relationship between remotely sensed data and object (i.e. specific LULC on the ground).

Accordingly, GCPs was collected from field survey and base map, then exporting the point to ArcGIS by connecting google earth to shows similar land cover type. This point has been taken by applying a stratified random sampling method at field site. Such points were collected using global positioning system (GPS) instrument for individual LULC classes. Different literature indicates that there is no exact guidance for total sample point taken for image accuracy. But the total sample training point should be taken at least ten times the number of pixel groups (10n) based on literature. The number of pixel groups in this study are six such as agriculture, forest, settlement, shrubland, grassland and bareland. Since, more than 390 point were used for image validation. Out of 390 point, two-third (2/3) of them were pinpointed from google earth and the rest of one-third were taken from field work.

Additionally, GCPs was used to produce signature for supervised classification and accuracy assessment of satellite images in the watershed.

3.2.1.2 Satellite Image Processing

Remote sensing is systems used for analysis of image in particular study. The satellite image downloaded from USGS website (https://earthexplorer.usgs.gov) at free charge for the proposed period of land scenarios (1989,2002, 2011 & 2019). The selection criteria of the images have been taken based on no cloud cover (less than 10% coverage) at the study area, the images were fulfilling good quality according to the USGS rating scale, the resolutions of the images were similar and the images were cover the similar period as the meteorological data time series. All images acquired in the month of November, December, January & February to get high quality with less or no cloud cover. The image is radiometrically and geometrically corrected since it is a level one product. Atmospheric correction had never been applied in this study because of the images were free from cloud exposure and the adopted classification and post classification comparison (PCC) approach compensated for the variation in atmospheric conditions. The images included the visible (bands 1, 2 and 3) for Landsat 5 TM, (bands 1, 2 and 3) for Landsat 7 ETM+ and (bands 2, 3 and 4) for Landsat 8 (OLI_TIRS), the near infrared (NIR), shortwave infrared (SWIR), and middle infrared (MIR) bands with 30m spatial resolution. Hereafter, the image has been processed using the support of ERDAS IMAGINE version 2014 and ArcGIS software.

Table 3.2 Satellite image data

S. N	Name	Year	Acquisition Date	Spatial Resolution	Band Number	Path/Row
1	LANDSAT_5 TM	1989	Feb 23, 1989	30mx30m	7	167/55
2	LANDSAT_7 ETM	2002	Nov 18, 2002	15mx15m	7	167/55
3	LANDSAT_7 ETM	2011	Dec 29, 2011	15mx15m	7	167/55
4	LANDSAT_8 OLI	2019	Jan 25,2019	15mx15m	11	167/55

All satellite image listed above table have been downloaded from https://earthexplorer.usgs.gov website.

LANDSAT_7 ETM of 2011 historical times have problems during scanning the images. The scan gap interpolation has 2m in the image. This scan gap forms headline on the image which marks to hide the visibility of exactness of image classes and thus gap must be corrected for accurate classification of images. Therefore, using QGIS tools headline forms on the image has been removed.

3.2.1.3 Land-use/Land Cover Classes

The LULC classes were identified for 31 years over the past time in the study area. The selection criteria of classes were taken depend on homogeneity of the image location at least 60mx60m in size to confirm identical pixel groups under sample training sets. The image classes were classified by ERDAS IMAGINE 2014 version. An arrangement of image classes could be evaluated by using merging techniques into the same LULC categories based on visual observation at field level and google earth pro, literature review (information obtainable from MWRIE) and previous knowledge on the study area. The total of LULC classes were assessed into six dominant groups in this study area. Each of class was described in table 3.3.

Table 3.3 Overview of LULC classes at Shaya watershed in the past time

LULC Class	Description
Agriculture	Includes cultivation land and crops area that farmers will use for production purpose.
Forest	Comprise mixed, dense, sparse forest with the plantation of trees by human.
Shrubland	Remnant forest which doesn’t destroyed by human activities and uncultivated land.
Grassland	Areas occupied by small ranges that used for animal grazed.
Settlement	Area covered by small village, town in which people have been lived.
Bareland	Areas with no dominant vegetation cover at least 90% of the area, rock and erodible soil layer and river channel.

The principal LULC classification methods are unsupervised and supervised classification method. In this paper, supervised classification methods have been considered for classification of LULC classes due to its better accuracy (for detail information, see literature in chapter-2).

3.2.1.4 Supervised Classification

The supervised classification approach requires prior knowledge about land cover types that are to be classified and mapped (Santillan et al., 2011). In this classification techniques, to get better results larger training sets has been used (Myburgh and Van Niekerk, 2014). Gumindoga et al. (2014) describes selection of sample training points is based on the relative proportion of each LULC type derived from visual interpretation of the image with respect to ease of survey, variety of features present, weather condition and etc. The maximum likelihood classification (MLC) is one of the most common popular methods of supervised classification technique (Santillan et al., 2011). This method is familiar for its ability to establish good separation between classes and improving the accuracy of classification (Thakkar et al., 2015) and also uses the means, variances of the training data to estimate the probability that a pixel is a member of a class (Ayele et al., 2018).

3.2.1.5 Accuracy Assessment

Accuracy assessment is an essential step in the process of analyzing remote sensing data. It uses to determine the degree of 'correctness' of classified image. Overall accuracy is one of the basic accuracy measures. This accuracy is calculated by dividing the correctly classified pixels (sum of the values in the main diagonal) by the total number of pixels checked. Two approaches are there in accuracy assessments: such as user's accuracy and producer's accuracy.

The producer's accuracy is derived by dividing the number of correct pixels in one class divided by the total number of pixels as derived from the total reference data column. It includes the error of omission which refers to the proportion of observed features on the ground that are not classified in the map. The more errors of omission exist, the lower the producer's accuracy.

Mathematically, Producer's accuracy (%) = 100% − error of omission (%)

User's accuracy is determined as the correct classified pixels in a class divided by the total number of pixels that were classified in that class. The user's accuracy is, therefore, measure the reliability of the map. It informs for users how well the map represents what is really on the ground. One class in the map can have two types of classes on the ground. The 'right' class, which refers to the same land cover-class in the map and on the ground, and 'wrong' classes, which show a different land cover on the ground than predicted on the map. The latter classes are referred to as errors of commission.

Mathematically, User's accuracy (%) = 100(%) − error of commission (%).

Kappa is measure agreement between the classification map and the reference data. Higher values of kappa indexes indicate higher agreement between the actual and the simulated maps.

Kappa values > 0.80 characterizes as high classification performance, between 0.40 - 0.80 indicate moderate classification performance and Kappa values < 0.40 indicate poor classification performance (Lillesand et al., 2008).

Mathematically, $k = \frac{po-pc}{1-pc}$ …………………… (equation 4)

Where, Po: the proportion of observed agreements, Pc: proportion of agreement expected by chance. In this paper, results were shown in annex-A.

3.2.1.6 Land-use/Land Cover Change Detection

After the proposed land maps (1989, 2002, 2011 & 2019) were classified independently, then the detection of LULCC had been assessed in this research work which is one of objective. The change detection provides the size and distribution of changed area (either negative or positive). This change detection can help to compare and analyze the impact of LULC change on water balances. The post-classification method has been applied for the change of LULC detection. In this method, merging very small size of image classes into neighboring of large sized images with similar pixel groups were vital for detected image class types without difficulties. Because of this method, doesn't need to have for co-registration of the image, and has low sensitivity to spectral variation; it also provides a ''from-to'' change information (Raja et al., 2013). The final LULC change detection were mapped for three date ranges (1989-2002, 1989-2011, and 1989-2019) by using ArcGIS software.

3.2.2 Land-use/Land Cover Changes Response to Water Balance Components

The effects of LULC changes on WBCs have been analyzed by modeling approach using the QSWAT model in this particular study area which is a part of research objective work. In this part, the water balance variable was mapped with respect to four land maps. The result has been determined on annual mean of rainfall- runoff processes under sub-watershed scale.

3.2.2.1 QSWAT Model Setup

The required input data for QSWAT model were listed in the following table.

Table 3.4 Input data of QSWAT model

Input Data	Description	Source
DEM	DEM was used for delineate watershed boundary, stream network, drainage density, slope and elevation, and used to compute the hydrological response units (HRU)	EGSII
LULC map	This map was organized based on proposed land maps (1989, 2002, 2011 & 2019) to evaluate LULC change detection and to simulate WBCs	USGS website
soil map	Characteristics of soil was organized for each of soil units in the form of polygon shape file to simulate WBCs	EMWIE
Metrological data	This were arranged either from measured data set or weather generator model (WGEN) like relative humidity, sunshine hour and solar radiation in the form of text file to simulate WBCs	ENMA

The General procedure of QSWAT model setup was described in the following steps:

1. Watershed delineation

The Watershed boundary was delineated from the gridded file of the DEM. The soil map, LULC map, and the DEM were projected into the same projection called UTM Zone 37N, which is the projection parameter of Ethiopia. The Watershed delineation process includes five major steps, DEM set up, create a stream, outlet and inlet shapefile, watershed outlet selection, and calculation of sub-basin parameters. To create a stream network, threshold methods must be able to limit the minimum size of the sub-watershed. In this study, 13 sub-watersheds have been delineated by the QSWAT model for investigation of water balance simulation. Each of the sub-watersheds were delineated based on the direction of flow to streamflow channel with having similar soil type, land cover type, and slope.

2. Hydrologic response units (HRU) creation

HRU is defined as a watershed that has single soil, slope, and land use properties. This HRU was created by the QSWAT model using a land map, soil map, and slope of the watershed. Each of LULC and soil were overlapped, and multiple slope option (an option which considers different slope classes for HRU definition) was selected. The LULC, soil and slope were reclassified to correspond the parameters in the SWAT database. After reclassifying the land-use, soil, and slope in the SWAT database, all these physical properties made to be overlaid for HRU definition.

The HRU distribution in this study was determined by multiple HRU method for each of sub-watershed. In this step, a threshold level (10%, 8%, 10%) was used to eliminate minor land uses, soils, or slope classes in each sub-watershed respectively. This helps to study the changes in water balance components for various land covers, soils, and slopes (Bansode and Patil, 2016).

3. Setup and run

After creating HRU successfully, the edition and run model had been carried out. Under this, the project database was connected with the reference database (QSWATRef2012.mdb), then after meteorological data were inserted and run to executable forwards. Importing the output file to the database is the final step to ready the output in visualization forms.

4. Visualization

Visualization can allow output from the SWAT to be visualized graphically by sub-watershed, reach, and HRU. This visualization has three parts, namely static data, animation and plot. In the static data, the output of the SUB, RCH, or HRU was visualized in map forms as daily means, monthly means, annual means, maxima minima, and totally with respect to time. In the plotting part, the output of reach was sketched in the form of the line graph, histogram, and plotting values against time (observed flow with the simulated flow). In this study, the output of WBCs was displayed in map style via static data techniques in QSWAT.

3.2.2.2 Discharge and Precipitation Data

Discharge data were obtained from Ministry of Water, Irrigation and Electricity (MOWIE) in Ethiopia for one stream gauging station which is located near to Bale-Robe Town at side of bridge. This data was covered 26 (1989-2014) years for conducting the impact of LULC changes on streamflow. Understanding amount of streamflow available in the watershed enable for water resource development (e.g. constructing diversion structure like weir, dam a long river cross-section for irrigation, hydropower and water supply purposes). The quantity of streamflow is affected by climatic and land-use/land cover factors. In this study, streamflow change was evaluated after the quality of the hydrometeorological data had been checked that resulted from change of observer, instrument replacement old by new, technical faults during measurements and another factor. The missing value of hydro-metrological data was filled by average and multiple imputation techniques in SPSS and the consistency of them were done by double mass curve methods.

Precipitation data also collected from National Metrological Agency (NMA) of Ethiopia. The total four gaged station namely Goba, Rira, Bale Robe and Dinsho were considered for investigation of streamflow and water balances in this study. The size of data was varied between gaged station. Precipitation is the key element of hydrological components in the watershed which play great role in distributing its into surface runoff, lateral flow and ground water flow. So, understanding such variable are very essential to keep the health of the watershed.

The gauged station of precipitation is assumed as point-precipitation. To change it to areal precipitation, there are so many methods used to estimate areal average of precipitation over the watershed. The choice of method requires decision in consideration of quality and nature of data, and required precision of the result. In this study, the areal average precipitation of Shaya Watershed was determined by Theissen polygon methods using four station within or near the watershed as shown in the figure 3.7 below. The theissen polygon was created by using ArcGIS software.

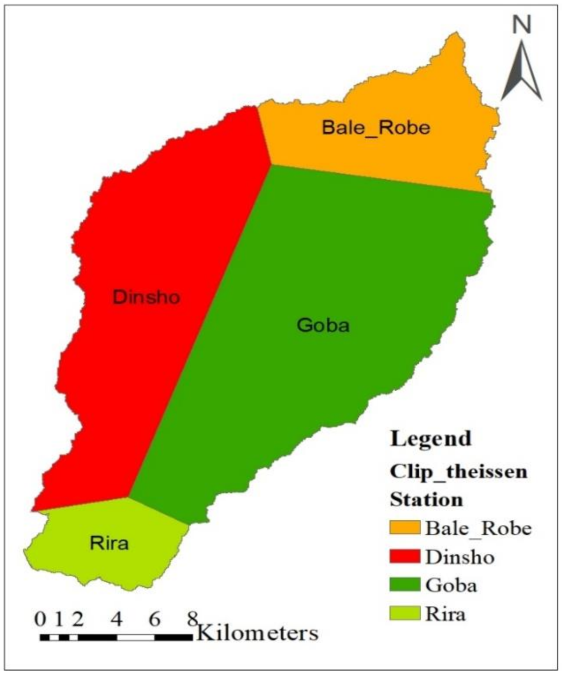

Figure 3.7 Theissen Polygon Method

Table 3.5 Areal coverage of Precipitation in Shaya Watershed

Station Name	Longitude	Latitude	Altitude	Areal coverage _km^2	Percentage (%)
Bale _Robe	40	7.133	2480	66	14.57
Dinsho	39.77	7.1	3072	143	31.57
Goba	39.98	7.02	2614	212	46.80
Rira	39.83	6.74	2700	32	7.06
Total				453	100%

The table 3.5 above revealed that the Goba station has covered large area (212km^2) while Rira station has covered small area (32km^2). Each station has their own contribution for surface runoff formation based on biophysical characteristics of the watershed.

Table 3.6 Summary of annual mean areal precipitation in Shaya Watershed

Station	Mean precip mm	Areal-coverage km^2	Mean-areal precip mm	Mean-annual precip mm/km^2
Goba (1997-2018)	947.7	212	200910.4	443.5
Rira (1989-2017)	866.2	32	27719.3	61.2
Robe (1989-2018)	840.1	66	55447.5	122.4
Dinsho (1989-2017)	1272.3	143	181931.0	401.6

Where, precip ----precipitation

3.2.2.3 Potential Evapotranspiration

Potential evapotranspiration (PET) is the total water losses exists in the watershed. PET can be affected by climatic factors like temperature, solar radiation, relative humidity and wind speed. It uses to identify the aridity indices of the watershed. An aridity index is defined as lack of long-term precipitation and it could be determined as the ratio of PET to P which has potential to shows the degree of drought, famine or normal condition of climates. In this study, PET was calculated by Penman–Monteith method using Bale-Robe principal station (Shao et al., 2018; Tesfahun and Dereje , 2019).

$$\mathrm{PET} = \frac{0.408 \triangle (\mathrm{Rn} - \mathrm{G}) + \gamma \frac{900}{\mathrm{T}+273} \mathrm{U2}(\mathrm{es} - \mathrm{ea})}{\triangle + \gamma(1 + 0.34\mathrm{U2})} \ldots \ldots \ldots \ldots \ldots \ldots \mathrm{equation}(5)$$

Where, PET=potential evapotranspiration(mm/day), Rn= net radiation at the crop surface (MJ/m^2/day), G=soil heat flux density (MJ/m^2/day), T=mean daily air temperature (°c), U2=wind speed at 2m height(m/s), es= saturation vapour pressure(kpa),ea=actual vapour pressure(kpa), es-ea=saturation vapour pressure deficit(kpa), △=slope vapour pressure curve(kpa/°c), γ=psychrometric constant(kpa/°c).

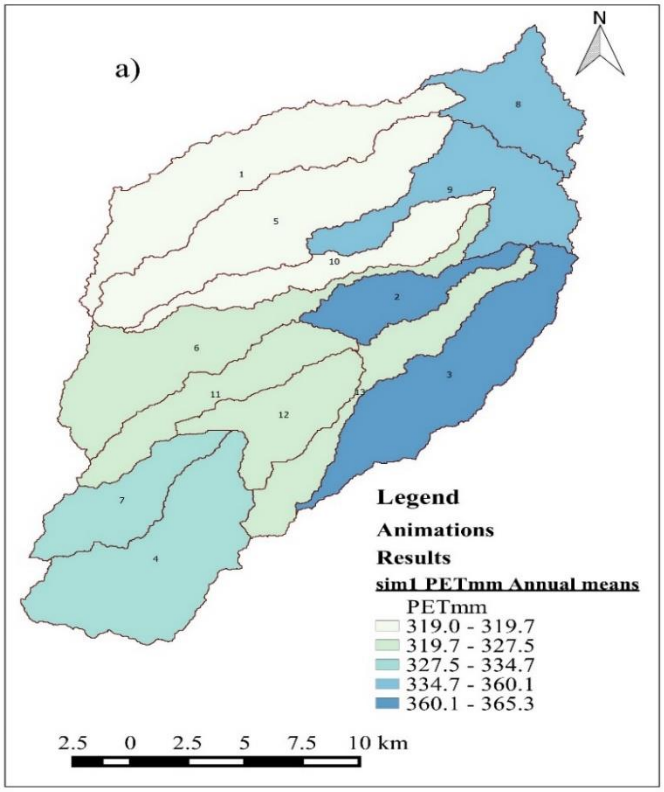

Figure 3.8 Potential evapotranspiration at sub-watershed scale for 1989 land map

Figure 3.8 above revealed that the annual mean value of PET in mm at sub-watershed level in Shaya Watershed. The range of minimum to maximum annual mean value of PET was (319-365.3mm) in the past 30 years. High PET was observed in northeast direction in area of more land covered by settlements and crop region. While low PET was seen at high rainfall region with high altitude (i.e. cool air could be reduced more water losses).

3.2.2.4 Double Mass Curve Method

In this study, the Double mass curve analysis was carried out after filling the missing value of hydrometeorological data using average and multiple imputation techniques in excel sheet and SPSS tools. Double mass curve is used to test consistency of hydro-climatic data for analysis or design purposes. The consistency of precipitation data was examined by double mass curve as shown in figure 3.9 below.

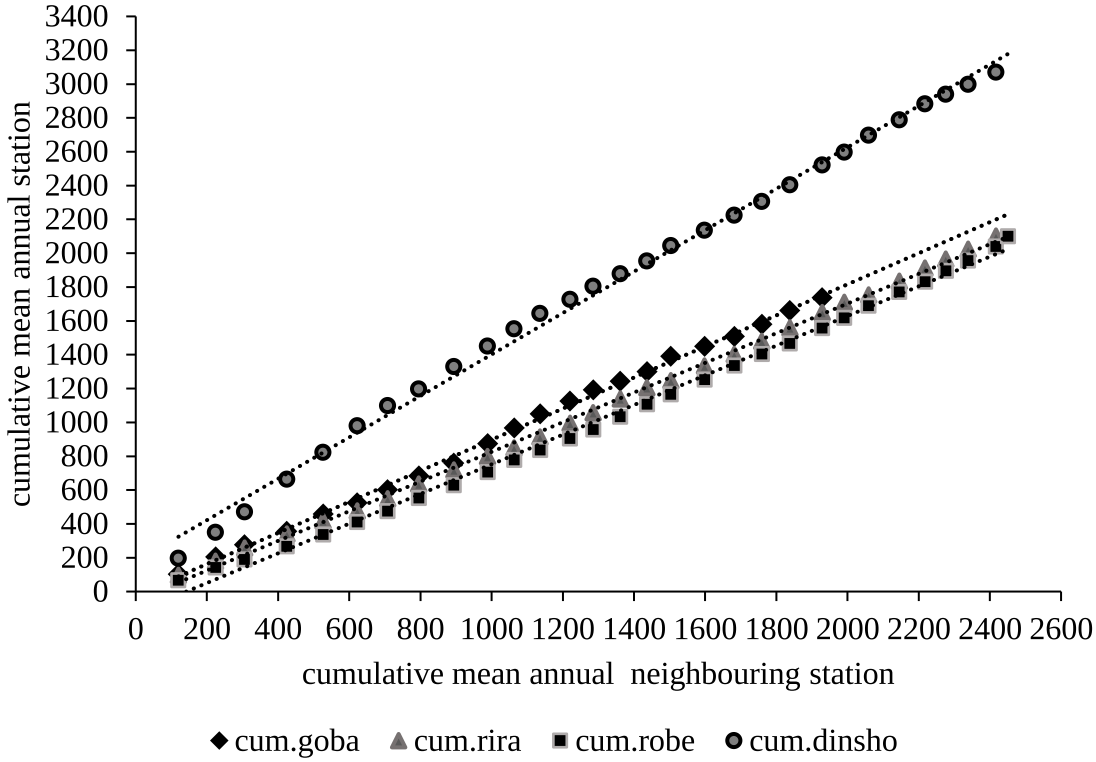

Figure 3.9 Double mass curve analysis (1989-2018)

3.2.2.5 Water Balance Estimation

In this study, the water balance variable has been estimated using QSWAT model by considering where land phase impacts on it. In this model, the water balance involves inflow, outflow, and storage. Precipitation(P) is the main inflow and evapotranspiration (ET), surface runoff (Qs), lateral flow (Ql), and base flow (Qb) are considered as outflow (Marhaento, 2018). QSWAT has four storages such as snowpack, soil moisture (SM), shallow aquifer (SA), and deep aquifer (DA). Snowpack is ignored due to it is not relevant in this study. Before precipitation reaches to ground surface, losses of water begun from vegetation parts which is called the interception processes. Hereafter, the rainwater infiltrates into soil strata and this movement of water is known as infiltration. Some portion of water percolates via shallow aquifer and remains others go too deeply recharged in the deep aquifer (see figure 3.11).

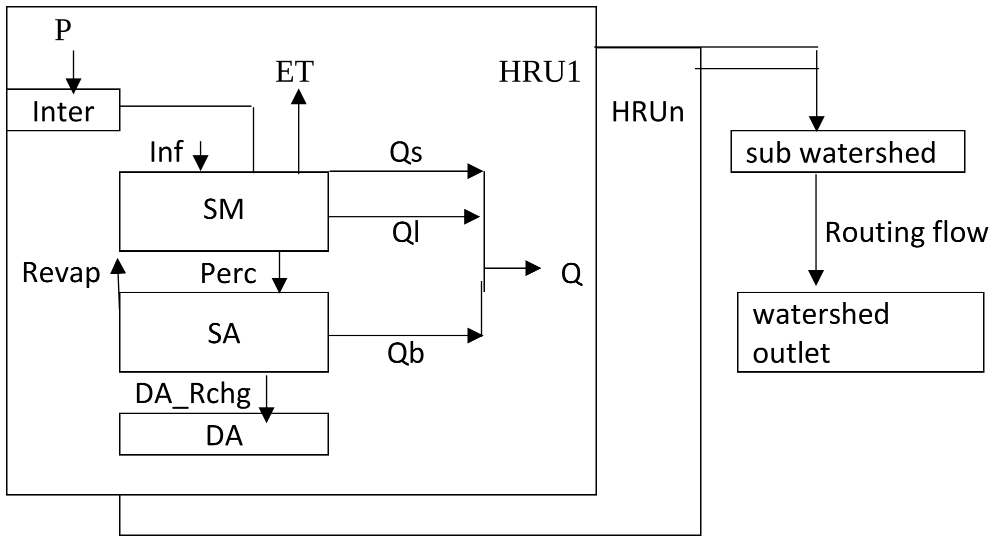

Figure 3.10 The QSWAT Model Structure

Where: P = precipitation, ET = evapotranspiration, Qs = Surface runoff, Ql = lateral flow, Qb = baseflow, Q = stream flow, SM = soil moisture, SA = shallow aquifer, DA = deep aquifer, Inter = interception, Inf = infiltration, Perc = percolation, DA_Rchg = deep aquifer recharge, HRU = hydrologic response unit, Revap = evaporation from shallow aquifer to soil moisture

To compute water balance component, spatial data of land, soil and slope are essential inputs of QSWAT model. The data were prepared according to model formats. The land and soil code for the QSWAT model were adjusted based on information wanted by the model to simulate the required outputs.

Table 3.7 Soil and Land-use code were used in QSWAT model to simulate water balances

Value	Soil code	Name	Value	Land-use code	Name
1	CMd	Dystric cambisol	33	URBN	Settlement
2	CMe	Eutric cambisol	37	BARR	Bare land
3	CMx	Chromic cambisol	49	FRST	Forest
4	LVh	Haplic luvisol	51	SHRB	Shrub land
5	LVv	Vertic luvisol	70	GRAS	Grass land
6	RG	Regosol	134	AGRL	Agriculture

3.2.2.6 Sensitivity Analysis

It is important in processing the hydrologic model and determining the main parameter in WBCs response to LULC impacts at the watershed level (Kamali et al., 2017). Hence, it helps during calibration and validation of the observed and simulated data to be well fit or close to an agreement with each other for decision-making in water resource planning and strategy. SWAT-CUP was an essential tool to fix the most sensitive parameter and calibrate or validate the observed hydrological data in the study area.

3.2.2.7 Model Calibration and Validation

Two-thirds (2/3) of monthly streamflow data from the total available of observed discharge were used for calibration and the remains of streamflow data (i.e. 1/3 of discharge data) used for validation. Both calibration and validation were done by using the combination of automatic and manual techniques. In this study, SWAT-CUP model has been used for calibration by adjusting model parameters to corresponding the observed and simulated streamflow data as much as possible, with a limited range of deviation accepted. The process could be taken between 100-500 simulation trials until it finds the best parameter set. Therefore, calibration would be stopped after checking R^2 and NSE values attain at least until the minimum recommended value (i.e. $R^2>0.6$, NSE>0.5, and PBIAS< ±25% (Arnold, 2015).

3.2.2.8 Model Performance Evaluation

For evaluation of model performance, Da Silva et al. (2015) describes model evaluation guidelines for quantification of accuracy in watershed modeling. The evaluation can perform by visual and statistical comparison of the observed and simulated streamflow data. However, the statistical criteria were used to evaluate the performance of the model. Such as Nash-Sutcliffe efficiency (NSE), percent bias (PBIAS), determination coefficient (R^2) and etc. They are used to evaluates the best fit either observed discharge data agree with simulated discharge data or not. The following table indicated that the equation and performance rating scale is stated for recommended statistics in the monthly time step (Da Silva et al., 2015).

Table 3.8 Model Performance Criteria

Equation	Performance rating scale			
	Unsatisfactory	Satisfactory	Good	Very good
NSE= $1-\frac{\sum_{i=1}^{n}(Qo-Qs)^2}{\sum_{i=1}^{n}(Qo-Qo.m)^2}$	$\leq$ 0.5	0.5-0.65	0.65-0.75	0.75-1.0
$R^2=\frac{[\sum_{i=1}^{n}(Qo-Qo.m)(Qs-Qs.m)]^2}{\sum_{i=1}^{n}(Qo-Qo.m)^2*\sum_{i=1}^{n}(Qs-Qs.m)^2}$	<0.5	0.5-0.6	0.6-0.7	0.7-1.0
$\text{PBIAS}=\frac{\sum_{i=1}^{n}(Qo-Qs)}{\sum_{i=1}^{n}(Qo)}*100$	$\geq \pm$25%	$\pm$15 - $\pm$25%	$\pm$10$\pm$15%	< $\pm$ 10

Where, NSE=Nash-Sutcliffe efficiency, R^2=Determination coefficient, PBIAS= percent-bias, and Qo, Qs, Qo, m, and Qs.m are observed discharge, simulated discharge, mean observed discharge, and mean simulated discharge in m^3/s respectively.

A smaller NSE value indicates a poorer fit between the simulated and observed data. It is possible to obtain a negative value of the NSE indicating that the average of the observational data provides a better fit to the data compared to the simulated data. So, when the value of NSE > 0.5, the model calibration and validation will be acceptable. R^2 indicates the linear relationship between simulated and observed data and ranges from zero (The model is poor.) to one (The model is good.). So, when the value of R^2 > 0.6, the model calibration and validation will be acceptable. PBIAS is describing the tendency of the simulated data to be greater or smaller than the observed data, expressed as a percentage. The optimum PBIAS value is zero and low values indicate that the model simulation is satisfactory. Positive values indicate a tendency of the model to underestimate while negative values are indicative of overestimation. This test is recommended due to its ability to reveal any poor performance of the model.

3.3 Research Flow Chart

General frame work formats for research work in propose study area are tabulated below in the form of sketch.

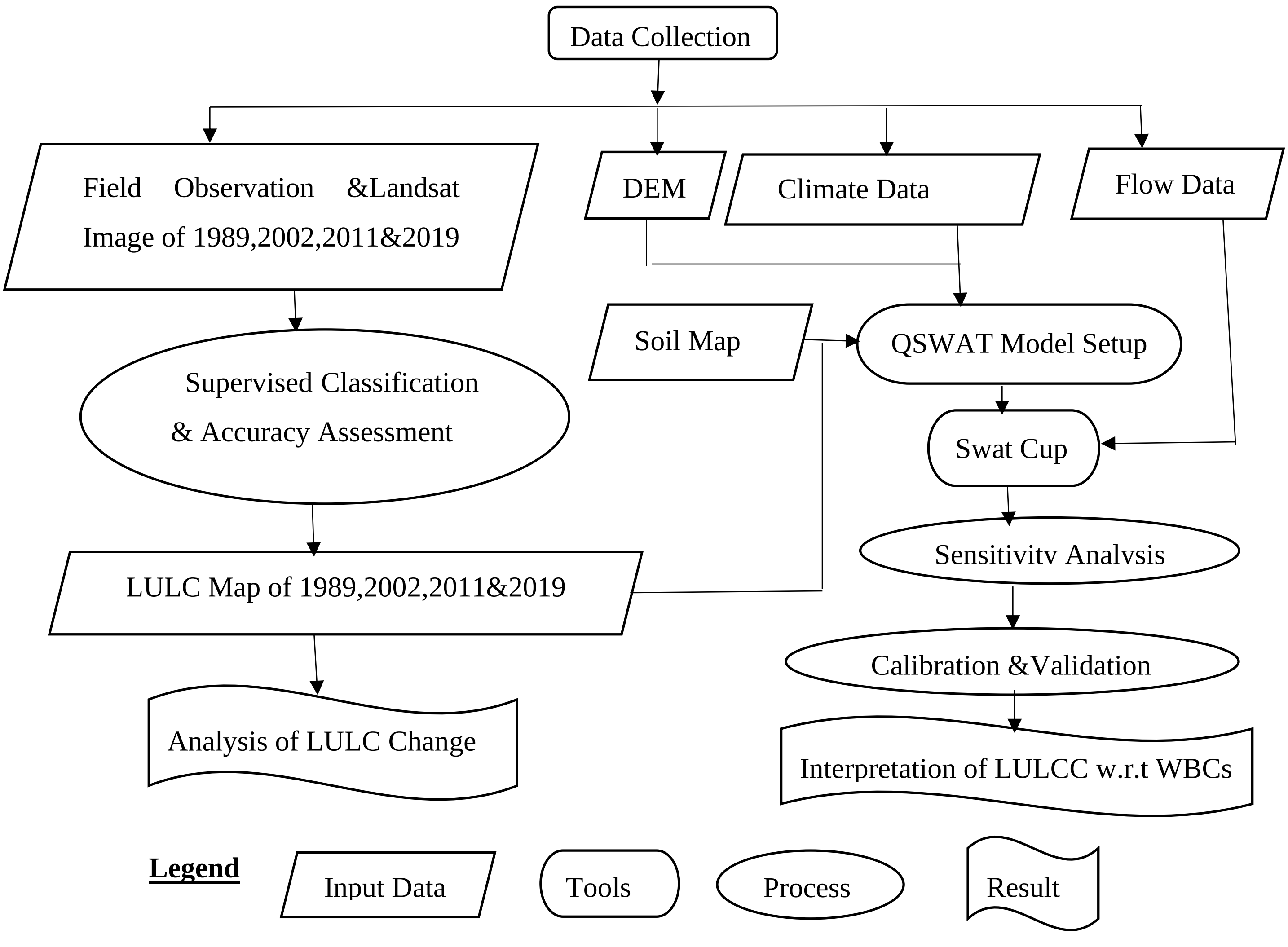

Figure 3.11 General frame work formats in the study area

4 RESULTS AND DISCUSSION

4.1 Land-use/Land cover Analysis

Under this study, the result of LULC classes has been analyzed in Shaya Watershed based on proposed land maps such as (1989, 2002, 2011 & 2019). The main LULC classes were classified by using visual observation, prior experience about the area, and information obtainable from MWRIE techniques. The main classes are agriculture, settlement, forest, shrubland, grassland, and bare land as shown in figure 4.1 below.

4.1.1 Land-use/Land cover Map

The dominant classes of LULC are crucial in terms of environmental resource management. Identifying particular classes of LULC has able to understand, control, manage, and execute decision-making processes for water resources development. The major classes were classified by ERDAS IMAGINE software and later the map was prepared using ArcGIS after post-classification techniques had been done. Figure 4.1 indicates the LULC map for historical land sat images (1989, 2002, 2011 & 2019) in the Shaya watershed.

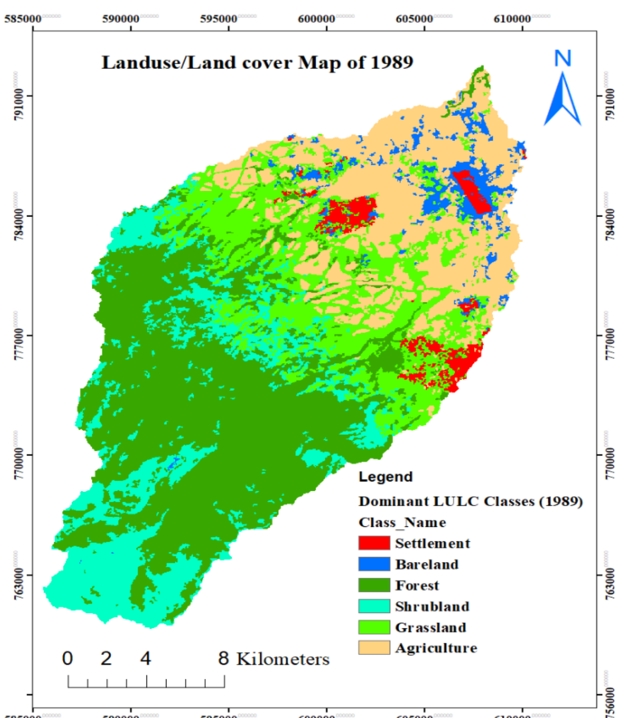

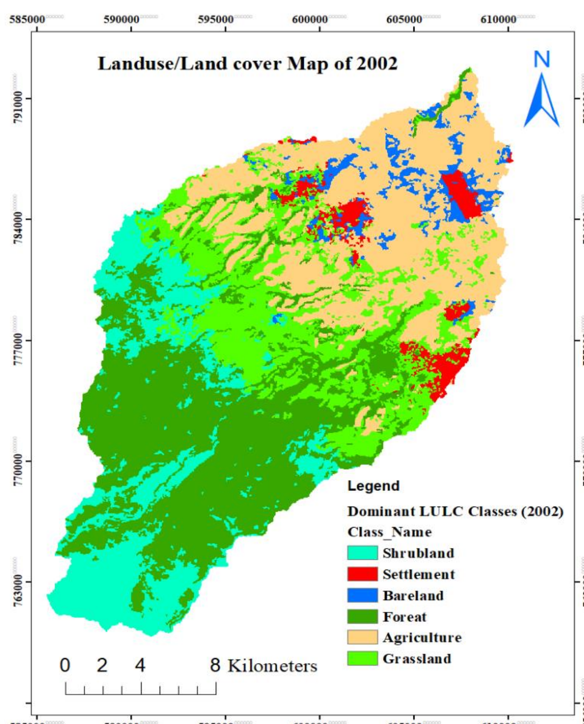

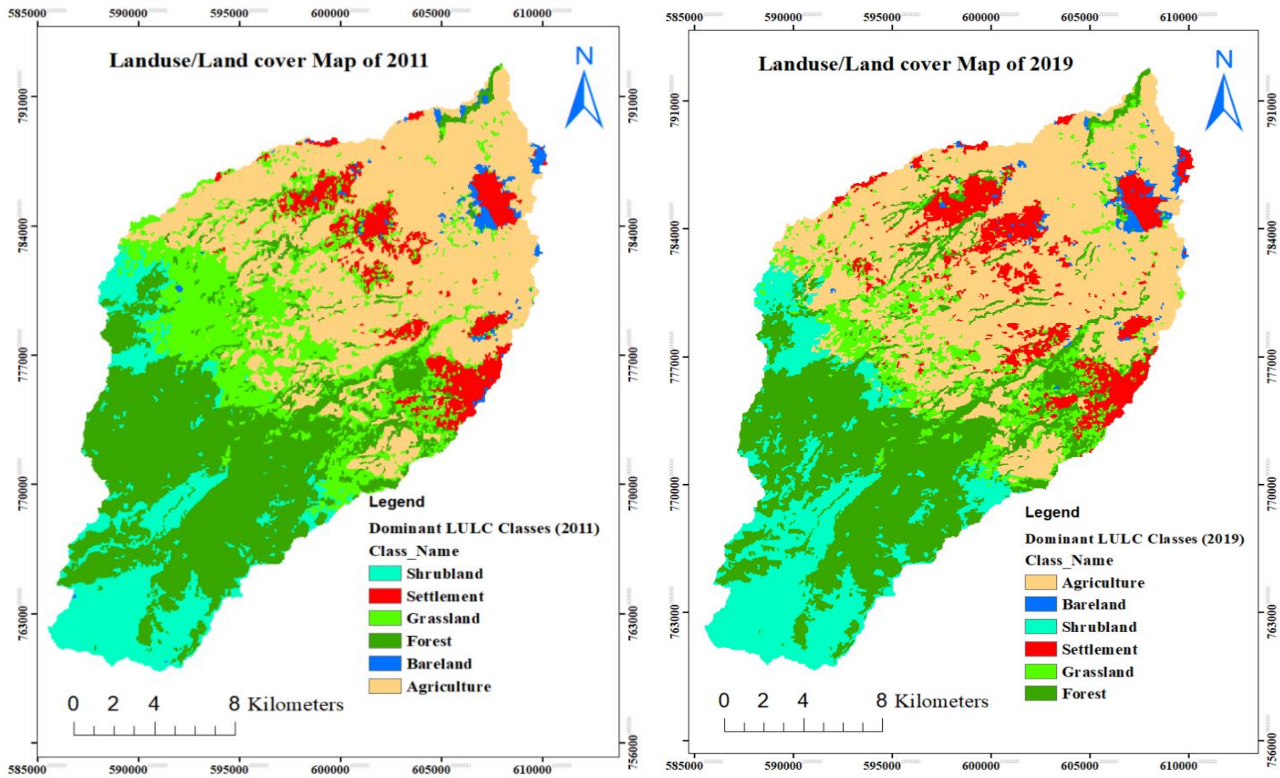

Figure 4.1 Dominant LULC Classes in Shaya Watershed for land maps 1989, 2002, 2011 &2019

Dominant classes were shrubland, settlement, grassland, forest, bareland, and agriculture as shown in figure 4.1. They have their own contribution to changes WBCs in the watershed through time series continuously. The size of each class can be varied and changed between land map scenario. Grassland has covered in the middle part of the watershed which had replaced gradually by agriculture and other classes. Agricultural practices have expanded from the downstream to the middle part of the watershed during the period of (1989-2019), while forest and shrubland decreased in the upper part of the watershed as rapidly and slowly in the same period. A decrement of forest, grassland and shrubland were expected to reduce ground water infiltration and rising overland flows (Marhaento, 2018).These are the impact of LULC change which deteriorate the living condition in the environmental. Therefore, the change of LULC should be control the amount of surface and groundwater in the watershed.

4.1.2 Quantification of land-use/land cover

The LULC classes found in Shaya Watershed has been evaluated from past historical Landsat image of (1989, 2002, 2011 & 2019) the year. The areal coverage of individual classes was presented in numeric and charts forms as a percentage (%). However, the output of each class was determined by MS-EXCEL as shown in table 4.1 and figure 4.2 separately. In 1989-year, the forest was covered 38.47% dominantly. Whereas, agriculture, grassland, and shrubland were covered moderately in the watershed as (20.41%, 18.80% & 16.55%) respectively. The minor LULC classes in the 1989 years were covered (3.26% &2.54%) by bareland and settlement.

Table 4.1 Summary of areal coverage in percentage of landuse/land cover classes

Class_Name	1989	2002	2011	2019	1989_2002	2002_2011	2011_2019	1989_2019
Agriculture	20.41	26.17	34.13	38.38	5.76	7.96	4.25	17.97
Bareland	3.26	3.30	1.12	1.12	0.04	-2.18	-0.01	-2.15
Forest	38.47	32.59	30.27	27.84	-5.88	-2.32	-2.44	-10.64
Grassland	18.80	18.58	16.81	8.92	-0.22	-1.77	-7.89	-9.88
Settlement	2.54	3.16	6.10	8.25	0.62	2.93	2.15	5.71
Shrubland	16.55	16.24	11.61	15.53	-0.31	-4.63	3.93	-1.02

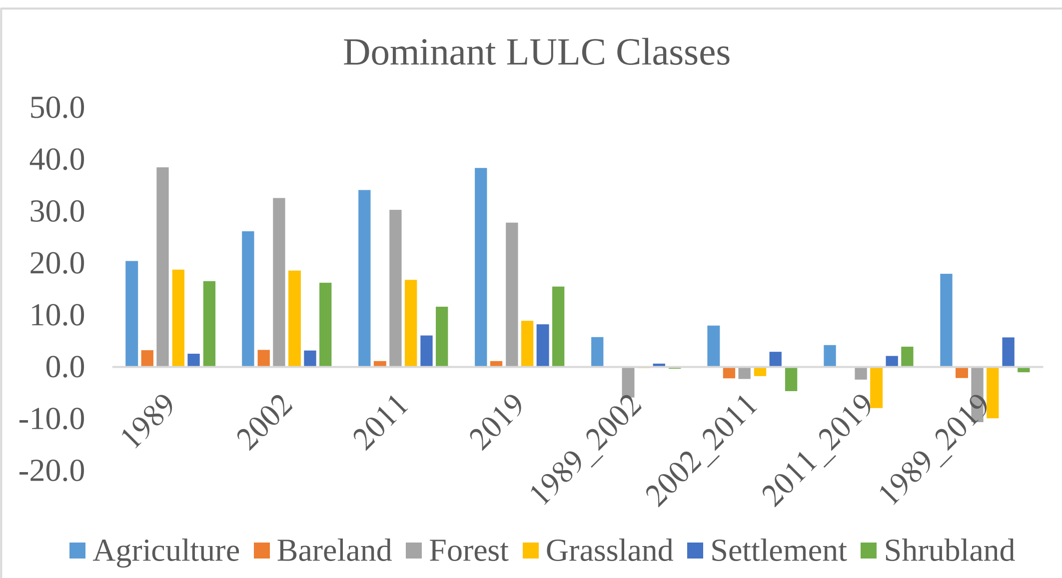

Figure 4.2 Summary of areal coverage in percentage of landuse/land cover classes

4.1.3 Land-use/Land Cover Change Detection

Dynamics LULC in the Shaya watershed were shown in figure 4.3 & table 4.2 in map & numerical forms respectively. The result of change detection was evaluated using the help of ArcGIS software and excel sheets for each conversion class. The map of change detection was derived as baseline (1989) to altered period (2002, 2011& 2019) of the LULC map techniques to get appropriate trends for each dominant class. From the viewpoint of the map shown below indicates that change and no-change of LULC classes. The white color represents as **no trend** occurs in each period of land scenarios (this means that the classes were constant throughout a time). The middle part of the watershed replaced by grassland and shrubland in the period of (1989-2002). Whereas the upper portion was mostly unchanged due to it covered by forest and shrubland in the same period.

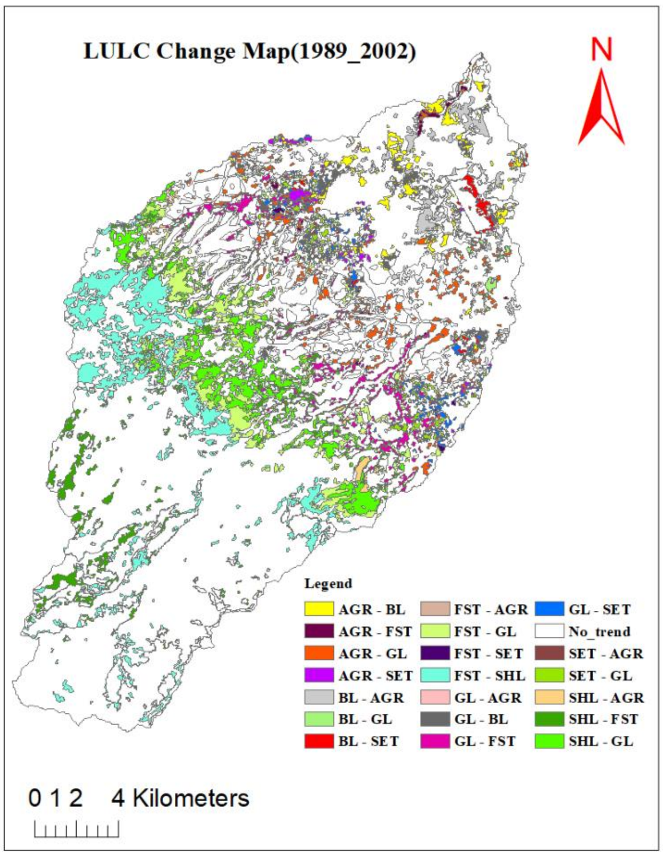

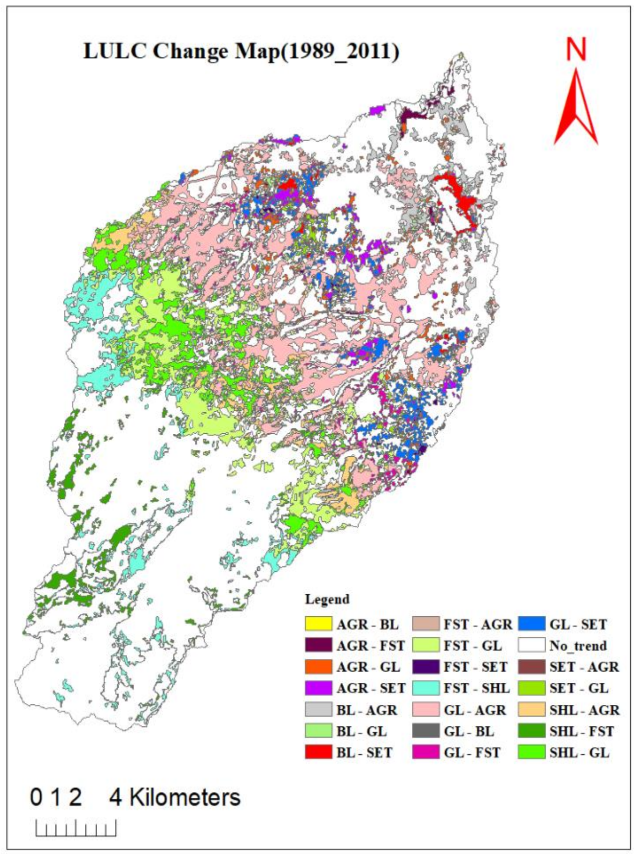

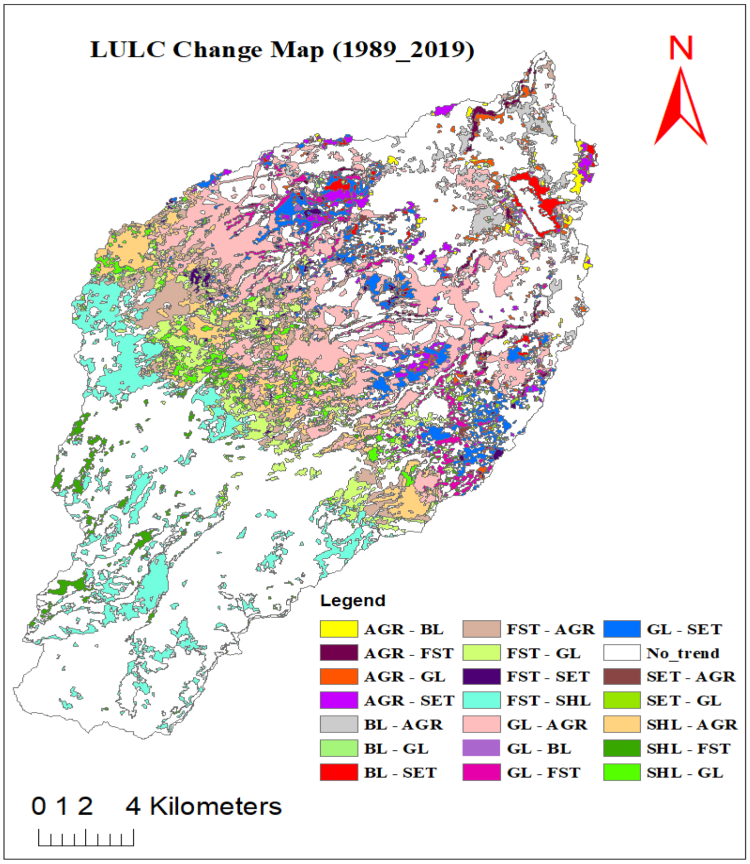

Figure 4.3 Dominant LULC classes altered ‘‘from-to’’ information for diverse land scenarios

In the period of (1989-2011) years as shown in figure 4.3 revealed that agriculture and settlement were covered in the middle-edge of the watershed. In the same way, some of the upper and downstream part of watershed were unchanged which is constantly covered by forest, shrubland and agriculture in the period of (1989-2019) years. The forest and grassland were dominantly decreased as agriculture, settlement and shrubland increased between 1989 and 2019 years.

In table 4.2 shown below revealed that in a period of (1989-2002) years, forest was converted into shrubland and grassland extremely as 5.69% & 3.5% respectively. Grassland was changed into agriculture by 7% which indicates more changes had been seen as comparing with other classes in the period of (1989-2002) years. During the period of (1989-2011) years, the higher trend was occurred in that of grassland which replaced by agriculture as 10.89% and forest into grassland by 6.38%.

Approximately 11.45% of grassland has been dominantly changed to agriculture during a period of (1989-2019) years. In the same period of the year, forest could be replaced by 6.45% into shrubland and shrubland also converted into agriculture by 4.24%.

Generally, the changed process was resulted from urbanization processes, population increment, natural phenomena and socio-economic interactions which are developed throughout the time. The trend of decreasing forest, grassland and increasing agriculture are the major challenges in the watershed due to increments of human demands and population growth. These factors are the indicator of land use/landcover changes. Therefore, the study revealed that there were observed changes in the land-use/land cover at Shaya Watershed in past 30 years and needs an action to control the land cover/use changes by promoting land management strategies in the future time.

Table 4.2 Dominant LULC classes altered ''from-to'' information for diverse land scenarios

LULC classes	Changed to	1989_2002 Area_km^2	Percent (%)	1989_2011 Area_km^2	Percent (%)	1989_2019 Area_km^2	Percent (%)
AGR	BL	5.16	1.14	1.91	0.42	2.22	0.49
	FST	1.15	0.25	1.37	0.30	3.07	0.68
	GL	7.46	1.65	5.13	1.13	3.34	0.74
	SET	1.75	0.39	5.40	1.19	6.34	1.40
BL	AGR	6.05	1.33	8.29	1.83	8.15	1.80
	GL	1.23	0.27	1.00	0.22	0.59	0.13
	SET	1.59	0.35	3.21	0.71	3.87	0.85
FST	AGR	1.72	0.38	7.27	1.60	16.47	3.64
	GL	15.84	3.50	28.92	6.38	17.28	3.82
	SET	0.33	0.07	0.84	0.18	2.29	0.51
	SHL	25.79	5.69	15.84	3.50	29.10	6.42
GL	AGR	31.71	7.00	49.35	10.89	51.88	11.45
	BL	3.35	0.74	0.59	0.13	0.76	0.17
	FST	6.66	1.47	4.43	0.98	7.68	1.70
	SET	2.91	0.64	9.35	2.06	14.52	3.21
SET	AGR	0.71	0.16	0.46	0.10	0.73	0.16
	GL	2.17	0.48	1.66	0.37	0.77	0.17
SHL	AGR	1.45	0.32	10.62	2.34	19.19	4.24
	FST	8.97	1.98	9.67	2.13	5.81	1.28
	GL	17.30	3.82	17.93	3.96	8.03	1.77

Where: - AGR = Agriculture SHL = Shrubland
GL = Grassland BL = Bareland
SET = Settlement FST=Forest

4.2 QSWAT Model Output

Water balance components at Shaya Watershed has been conducted by using QSWAT modeling approaches depending on past land map scenarios (1989,2002,2011&2019). The output of water balances was simulated by combination of DEM, land, soil, slope, and meteorological data including precipitation(mm), temperature (^{0}c), relative humidity (%), solar radiation (MJ/m^2), and wind speed (m/s at 2m height). Examples of water balance components resulted from the QSWAT model are surface runoff (SURQmm), percolation (PERCmm), evapotranspiration (ETmm), potential evapotranspiration (PETmm), soil moisture content (SWmm), groundwater flow (GW-Qmm), lateral flow (LAT-Qmm), and water yield (WYLDmm) (see figure 4.7).

4.2.1 Sensitivity Analysis

Under this portion, the researcher focused on the sensitive parameter that aids to distinguish which parameter is more sensitive to alter the rate of flow over a long-term period in the watershed to emphasize the way to manage and monitor the LULCC in the region. So, before analyzing the output of WBCs, identifying the most important sensitive parameter are essential steps in this study. The parameter was identified by using SWAT-CUP tools under SUFI2 optimization algorithm techniques. The best selection parameter depends on the initial output of the model behavior. Accordingly, the parameter was selected by adjusting manual operation and visual observation of hydrograph with the similarity of stimulated flows (that is the mean & standard deviation of both observed and simulated flow attains similar value). Later, the parameter had been obtained after 120 simulation numbers processed with five iteration steps.

Table 4.3 Summary of most important sensitive parameter of Shaya Watershed

S. N	Parameter_Name	Fitted_Value	Min_value	Max_value
1	R__CN2.mgt	-0.31	-0.35	-0.17
2	V__ALPHA_BF.gw	-0.28	-0.52	0.14
3	V__GW_DELAY.gw	29.24	19.38	34.84
4	V__GWQMN.gw	0.09	0.04	0.28
5	R__SOL_AWC(..).sol	0.17	0.11	0.42

6	R__SOL_K(..).sol	15.90	11.89	20.25
7	R__SOL_BD(..).sol	1.10	0.97	1.11
8	V__SLSUBBSN.hru	49.62	47.77	64.21
9	V__OV_N.hru	5.21	3.24	6.74
10	V__ESCO.hru	0.53	0.53	0.68
11	V__SHALLST.gw	1321.83	967.70	1332.47

Note: V__means the existing parameter value is replaced by a given value

R__means the existing value is multiplied by (1+ a given value)

Table 4.4 Description and application of Selected Parameter

symbol	parameter name & unit	application of parameter
CN2	SCS runoff curve number	monitor water fraction to infiltrate into soil or to produce surface runoff as overland flow
ALPHA_BF	Baseflow alpha factor (days).	control GW flow response to changes in recharges
GW_DELAY	Groundwater delay (days).	control delay time of water leaving from soil layer &entering into shallow aquifer
GWQMN	Threshold depth of water in the shallow aquifer required for return flow to occur (mm).	monitor amount of water in shallow aquifer to form return flow.
SOL_AWC	Available water capacity of the soil layer.	monitor soil water storage from field capacity and wilting point of soil moisture
SOL_K	Saturated hydraulic conductivity.	monitor the amount of water enter into saturated zone
SOL_BD	Moist bulk density.	manage infiltration rate of water in the soil and capacity of soil moisture contents for plant growth
SLSUBBSN	Average slope length.	control surface water movement
OV_N	Manning's "n" value for overland flow.	monitor the concentration time of flow and slope of overland flow
ESCO	Soil evaporation compensation factor.	control evaporation demand of soil
SHALLST	Initial depth of water in the shallow aquifer(mm)	manage rate of flow in shallow aquifer

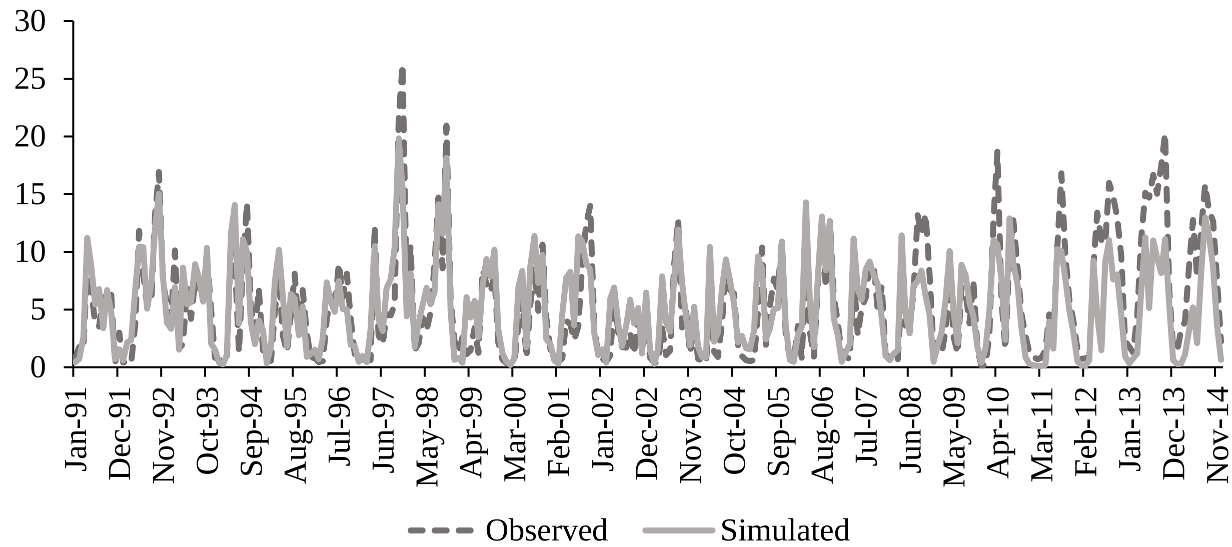

Figure 4.4 Monthly observed and simulated flow for long-term period (1991-2014)

As shown in figure 4.4 above, the simulated hydrograph was gradually decreased towards the end of the year as comparing observed flow because of the model performance efficiency decreases as the time series increases. The model performance was distorted in the long-term period to predict streamflow as close to actual flow, while the gap between lengths of land scenarios could affect the result of the model (e.g. as time series of observed flow were closer to the length of land scenarios, the greater accuracy of the model will predict flow too much closer to actual flow and vice versa).

4.2.2 Model Calibration and Validation

The calibration model was evaluated to approve the similarity of simulated flow with that of observed flow. The validation model was processed by using an independent set of flow data to verify the output of the model without further change of calibrated parameter. Both calibration and validation models were carried out monthly time steps from (1989-2014) years including two years warming up period (1989-1990) for land map (2002) scenario.

Table 4.5 Monthly streamflow calibration and validation for LULC map 2002

Condition	Period	R2	NSE	PBIAS
Calibration	1991-2005	0.74	0,73	-3.9
Validation	2006-2014	0.62	0.55	21.5

The colleration coefficient (r) of simulated and observed flow were (0.9 &0.8) in calibration and validation period as shown in figure 4.6. This is indicated as strongly associated between observed and simulated flow that existed both at calibration and validation period. The NSE value of monthly streamflow were 0.73 and 0.55 in calibration and validation period. In this case, the performance of QSWAT model during validation is found to be less accurate as compared to calibration period in monthly scale. But, the result of the performance is still satisfactory, which shows that the fundamental rainfall-runoff relationship and water balances including the intra distribution are well captured. Thus, results are within the range of good performance.

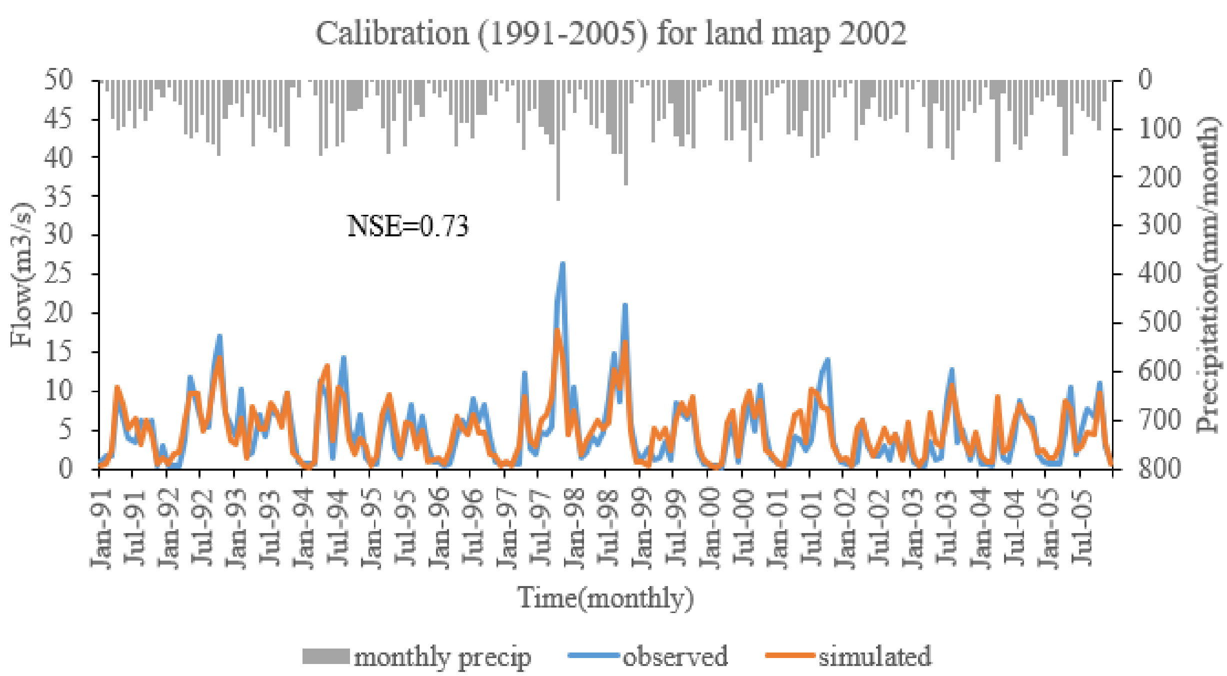

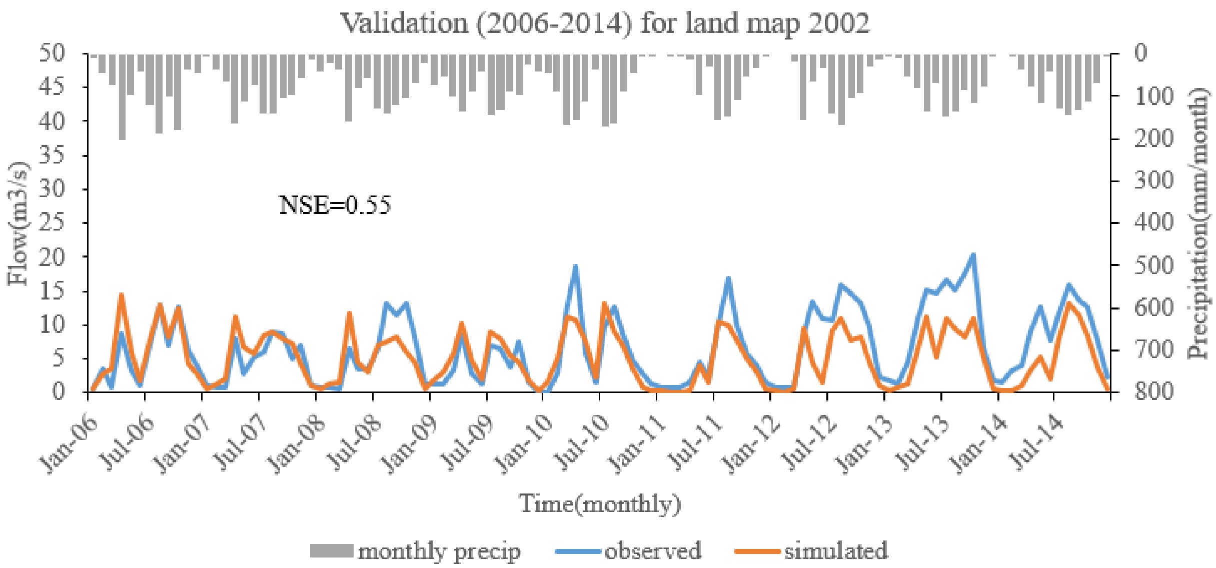

Figure 4.5 Calibration and Validation of observed hydrograph for land map 2002

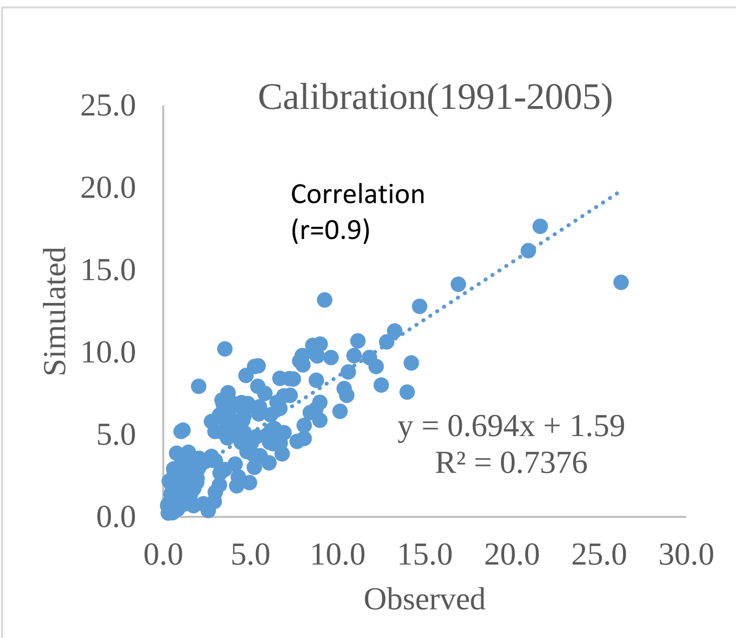

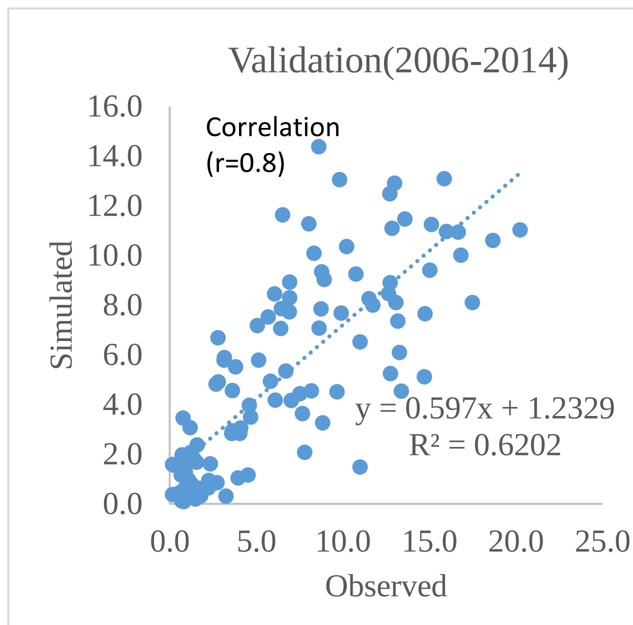

Figure 4.6 Scatter plot of observed and simulated flow at monthly scale

4.2.3 Effect of LULCC on Water balance components

In most cases, the LULC changes typically affect runoff yield, recharge, evapotranspiration, groundwater flow, water yield, and soil water moisture in watershed and sub-watershed level. These are leads to control water yield of surface river and groundwater aquifer which are very vital for ecosystem function and human use. Therefore, such the water balance components can causes impact on economic, social, and environmental degradation. To overcome such problems, it must be required to understand the impact of LULC changes on water balances by using semi-distributed model for adopt integrated watershed management after quantifying the rainfall-runoff formation. Hence, in this study, changes in WBCs were observed due to LULC changes as increment of deforestation, agriculture, population, and decrement of grassland happened in few past periods. The response of LULC changes to WBCs were assessed in terms of annual mean in form of maps as shown in figure 4.7 for each of land scenarios (1989, 2002, 2011, 2019).

From figure 4.7, the minimum and maximum value of ET were extended from (160-250 mm/year) at the sub-watershed level during the period of (1989-2019). The ET value was varied between sub-watershed and slightly increased year to year as a reason of water demand by the crop was increased as the agriculture area expanded in the last 30 years. Similarly, runoff vividly increases between (1989-2019) years in the watershed. This runoff was varied by (50-420 mm/year) at the sub-watershed level. This runoff yield was visualized in the north to west direction of the watershed in which high rainfall and more agricultural production has experienced in past few periods. In similar way, the groundwater flow was ranges as minimum and maximum from (240 - 610mm/year) at the sub-watershed level. This value of GW flow was fluctuated as a result of the density of LULC classes being varied at the sub-watershed level in past period (1989-2019).

The water yield was resulted from QSWAT model varied as lower to higher value from (480-910mm/year) at the sub-watershed scale in last three decades. This water yield is governed by land type coverage, soil, topography and others relative factors.

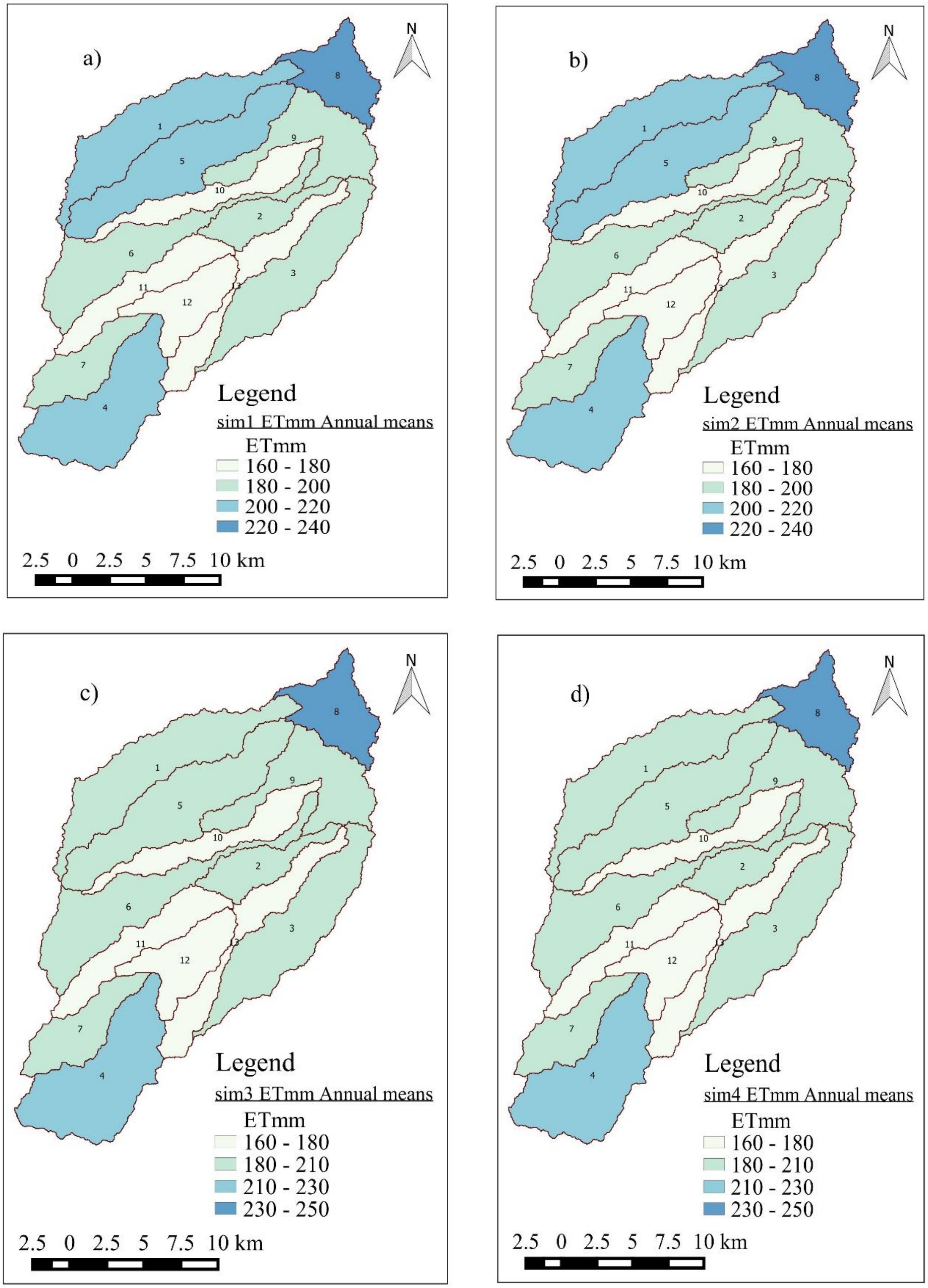
a)
N
Legend
sim1 ETmm Annual means
ETmm
160 - 180
180 - 200
200 - 220
220 - 240
2.5 0 2.5 5 7.5 10 km
b)
N
Legend
sim2 ETmm Annual means
ETmm
160 - 180
180 - 200
200 - 220
220 - 240
2.5 0 2.5 5 7.5 10 km
c)
N
Legend
sim3 ETmm Annual means
ETmm
160 - 180
180 - 210
210 - 230
230 - 250
2.5 0 2.5 5 7.5 10 km
d)
N
Legend
sim4 ETmm Annual means
ETmm
160 - 180
180 - 210
210 - 230
230 - 250
2.5 0 2.5 5 7.5 10 km

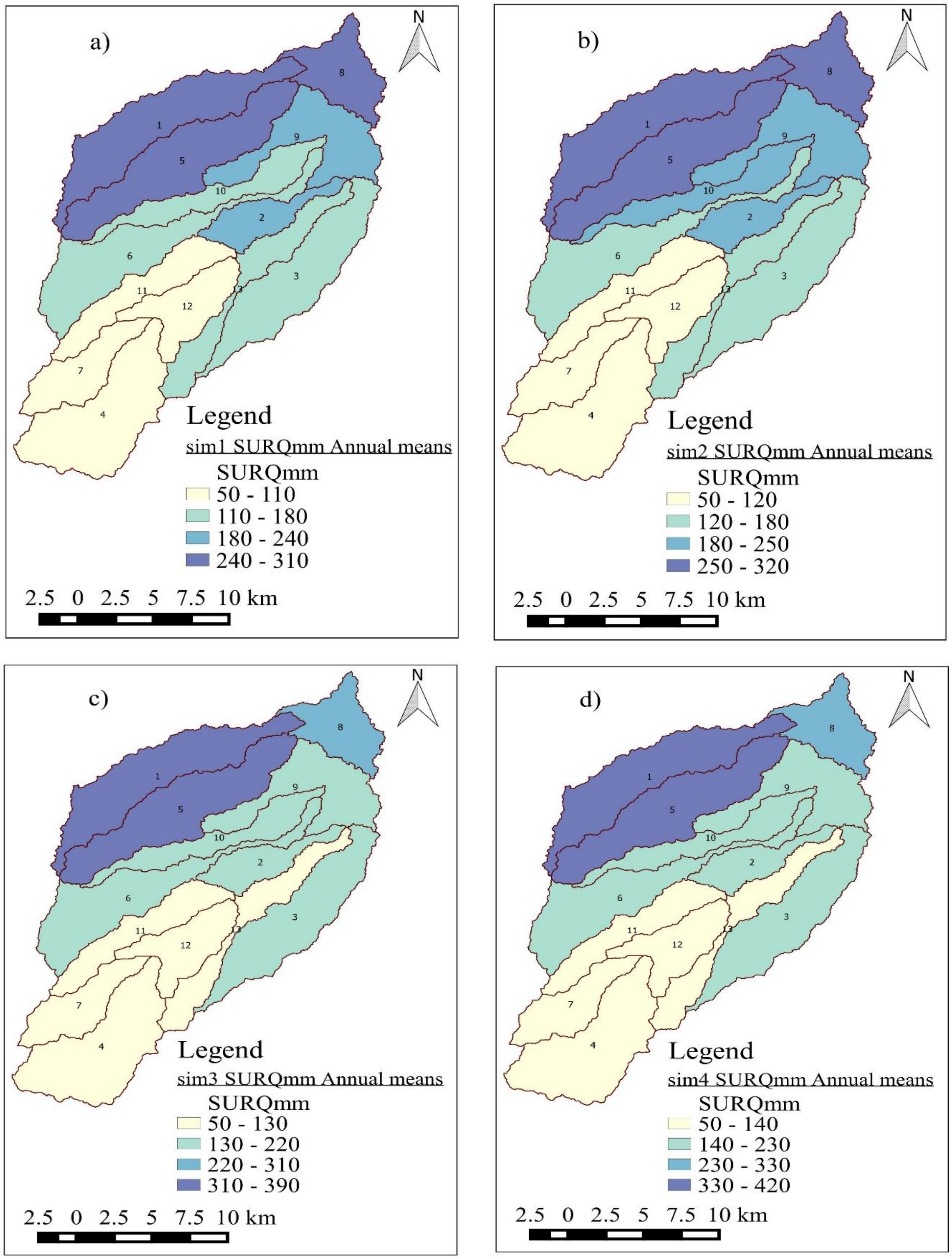
a)
N
1
5
8
9
10
2
6
3
11
12
13
7
4
Legend
sim1 SURQmm Annual means
SURQmm
50 - 110
110 - 180
180 - 240
240 - 310
2.5 0 2.5 5 7.5 10 km
b)
N
Legend
sim2 SURQmm Annual means
SURQmm
50 - 120
120 - 180
180 - 250
250 - 320
2.5 0 2.5 5 7.5 10 km
c)
N
Legend
sim3 SURQmm Annual means
SURQmm
50 - 130
130 - 220
220 - 310
310 - 390
2.5 0 2.5 5 7.5 10 km
d)
N
Legend
sim4 SURQmm Annual means
SURQmm
50 - 140
140 - 230
230 - 330
330 - 420
2.5 0 2.5 5 7.5 10 km

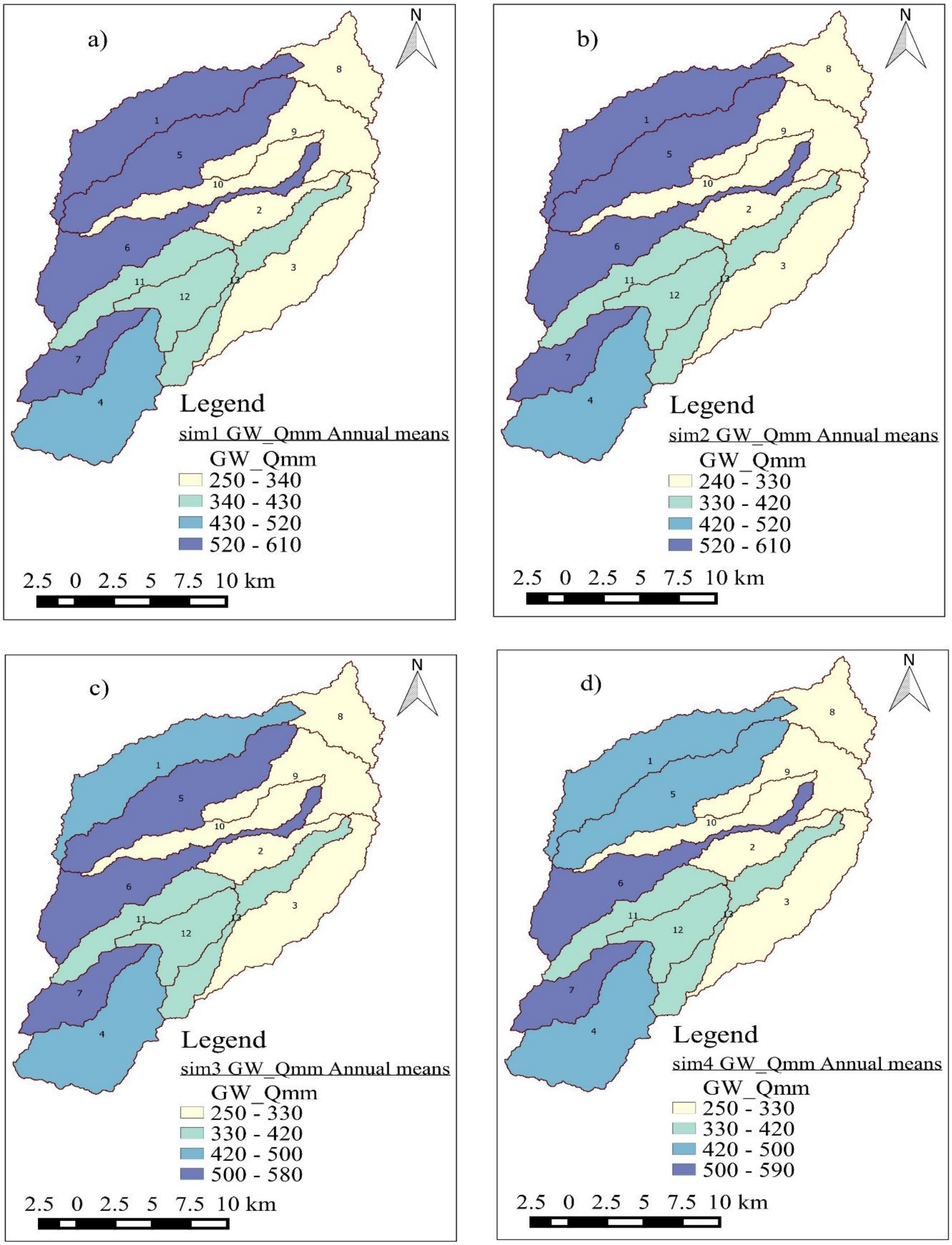
a)
N
8
1
9
5
10
2
6
11
13
3
12
7
4
Legend
sim1 GW_Qmm Annual means
GW_Qmm
250 - 340
340 - 430
430 - 520
520 - 610
2.5 0 2.5 5 7.5 10 km
b)
N
Legend
sim2 GW_Qmm Annual means
GW_Qmm
240 - 330
330 - 420
420 - 520
520 - 610
2.5 0 2.5 5 7.5 10 km
c)
N
Legend
sim3 GW_Qmm Annual means
GW_Qmm
250 - 330
330 - 420
420 - 500
500 - 580
2.5 0 2.5 5 7.5 10 km
d)
N
Legend
sim4 GW_Qmm Annual means
GW_Qmm
250 - 330
330 - 420
420 - 500
500 - 590
2.5 0 2.5 5 7.5 10 km

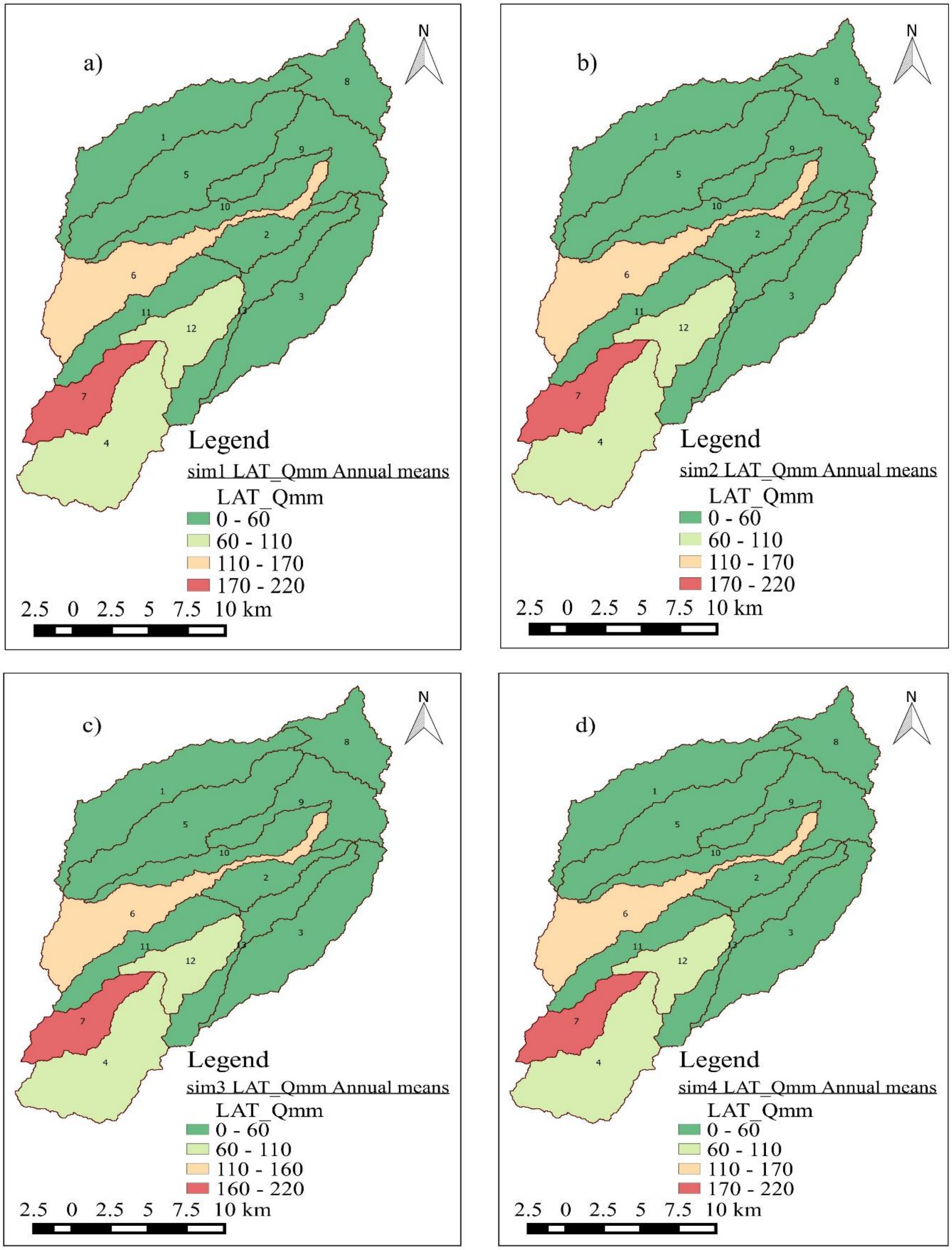
a)
N
1
2
3
4
5
6
7
8
9
10
11
12
13
Legend
sim1 LAT_Qmm Annual means
LAT_Qmm
0 - 60
60 - 110
110 - 170
170 - 220
2.5 0 2.5 5 7.5 10 km
b)
N
Legend
sim2 LAT_Qmm Annual means
LAT_Qmm
0 - 60
60 - 110
110 - 170
170 - 220
2.5 0 2.5 5 7.5 10 km
c)
N
Legend
sim3 LAT_Qmm Annual means
LAT_Qmm
0 - 60
60 - 110
110 - 160
160 - 220
2.5 0 2.5 5 7.5 10 km
d)
N
Legend
sim4 LAT_Qmm Annual means
LAT_Qmm
0 - 60
60 - 110
110 - 170
170 - 220
2.5 0 2.5 5 7.5 10 km

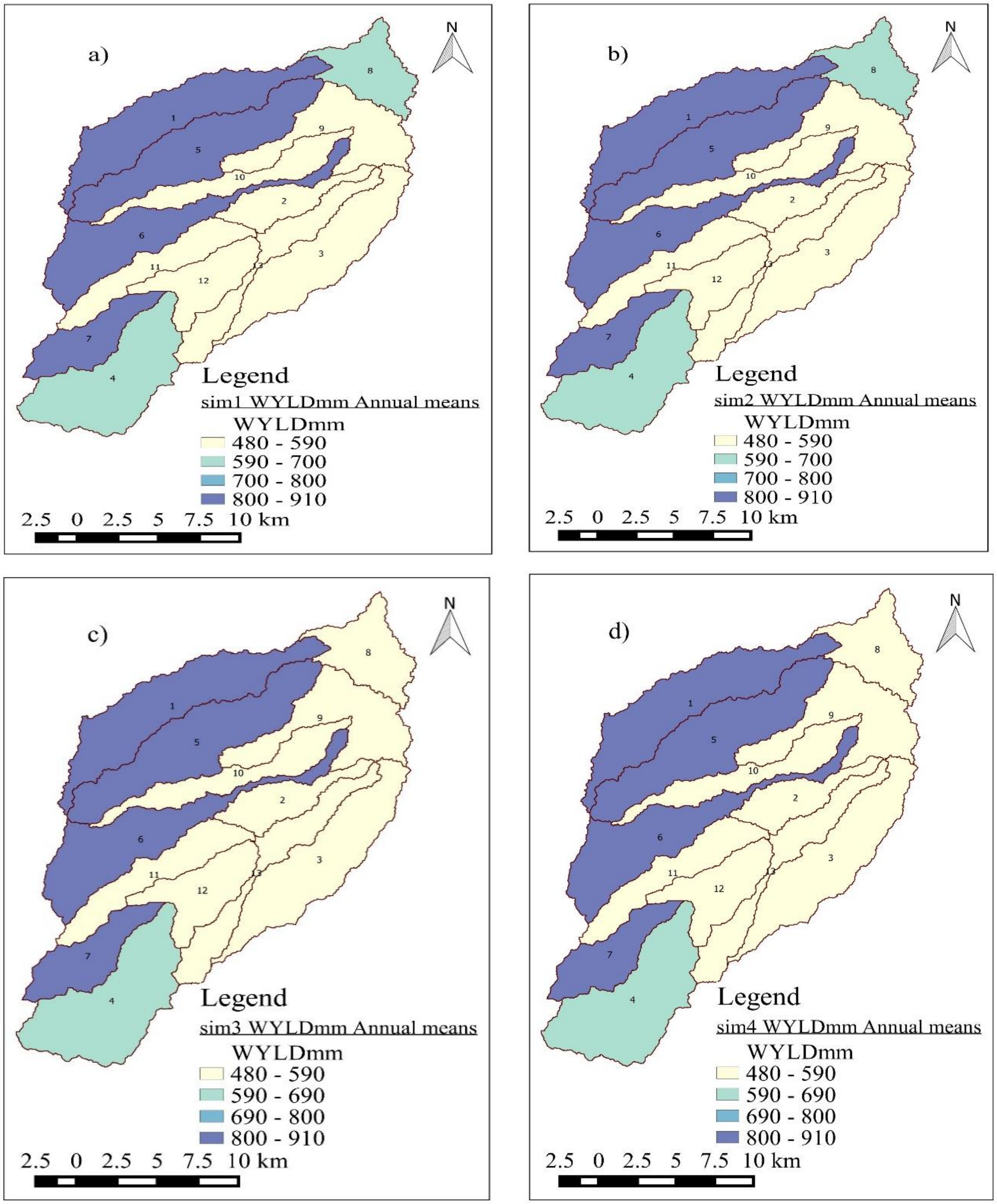

Figure 4.7 Water balance components at sub-watershed level under land maps a,b,c,d for (1989, 2002, 2011 & 2019) respectively.

Where: sim1, sim2, sim3 and sim4 are stands for simulated land map of 1989, 2002, 2011 and 2019 respectively.

4.2.4 Water Balance Coefficient

In this section, the water balance coefficients were measured such as streamflow to precipitation (Q/P), the ratio of evapotranspiration to precipitation (ET/P), surface runoff to streamflow (Qs/Q), base flow to streamflow (Qb/Q) and lateral flow to streamflow (Ql/Q) in the watershed using the base-altered mechanism. Streamflow or total flow at outlet of watershed is the summation of surface runoff, lateral flow and base flow.

Table 4.6 Percentage of water balance coefficient in Shaya Watershed under four land maps

WB ratio	1989	2002	2011	2019
Q/P	73.6	73.6	73.6	73.6
ET/P	23.3	23.3	23.4	23.4
Qs/Q	26.4	27.5	30.7	30.7
Qb/Q	65.0	64.0	61.1	61.1
Ql/Q	8.7	8.5	8.2	8.2

From table 4.7, the total precipitation has been contributed to streamflow and evapotranspiration as 73.6% and 23.3% respectively, while the remaining 3.1% of precipitation losses due to intercept by vegetation coverage in the watershed. The value of Qs/Q was increased from 26.4% to 30.7% in the period of 1989-2019, but Qb/Q was decreased by (65% to 61.1%) in three decades. However, slightly decreased changes were seen in Ql/Q as 8.7% to 8.2% during the period of 1989-2019.

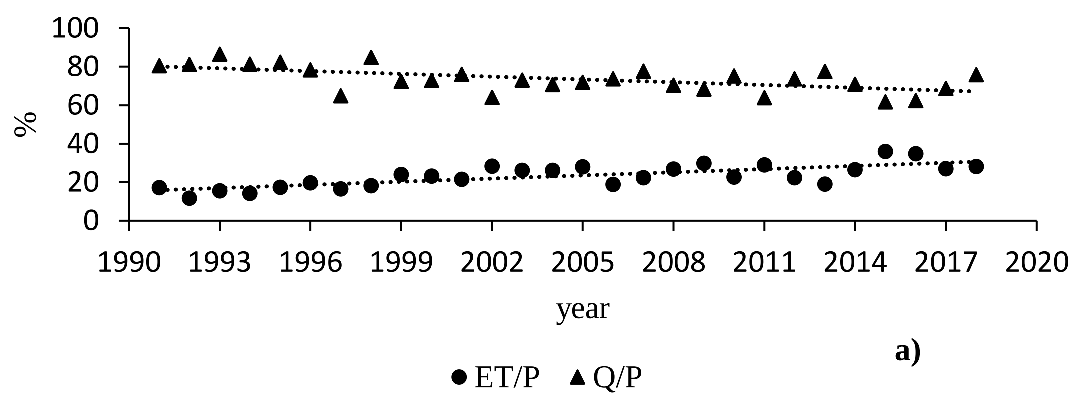

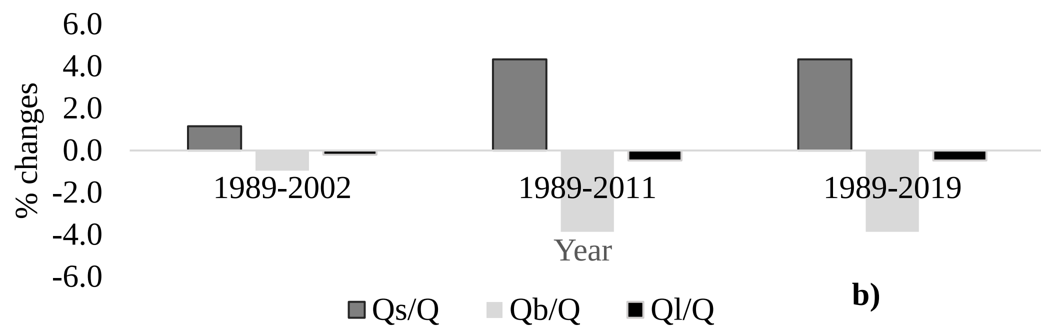

Figure 4.8 a) Simulated runoff coefficient and ratio of evapotranspiration to precipitation (ET/P) and b) Change of surface runoff to streamflow (Qs/Q), baseflow to streamflow (Qb/Q) and lateral flow to streamflow (Ql/Q) in long term period (1989-2019) in Shaya Watershed.

4.2.5 Annual and Seasonal contribution of LULC changes to Water balances

The ditributions of rainfall pattern in the Shaya Watershed is biomodial that is rain peakily during summer season from June to October month and short rains in belg time from March to May months. Rainfall is considered as inflow while evapotranspiration and stream flow are outflow to estimate water balances in the watershed. Under this portion, WBCs were estimated based on seasonal patterns in kiremt (Jul,Aug,Sep,Oct), bega (Nov,Dec,Jan,Feb) and belg (Mar,Apr,May,Jun). The graphical representation of water balance variables in the watershed can be detrermined depending on seasonal condition as shown in figure 4.9.

Runoff had increased between (1989-2019) in kiremt, bega, and belg by (14%, 2.8% and 10.1%) respectively. High runoff can occur in summer (kiremt) and low in winter (bega) season due to seasonal rainfall distribution was uneven and vary in the watershed. Approximately26.9% of surface runoff had been increased in the watershed during 30 years in past period. This change could being to be derived from combinaation of soil type, landuse/land cover type, topographic factors in the watershed.

However, groundwater flow and lateral flow were decreased successively in the four land scenarios. The high GWF and Ql has decreased by (11% & 1.5%) from (1989-2019) in kiremt season. In contrast, low GWF and Ql has decreased by (6.3% & 0.5%) in bega season.

Approximately (24.1% & 2.9%) of GWFand Ql had been decreased in the past 30 years. These changes being existed in the watershed as the result of decreased by (infitration rate of water) and increased (bulk density of soil).

Similary, evapotranspiration has slightly increased in seasonal distribution due to expanded agriculture were seen in past 30 years in the watershed. As well as, the high value of ET were observed in bega(winter) season due to high temperature and low rainfall had existed.

Total streamflow had been fluctuated in seasonal distribution as upward increased in kiremt and downward decreased in bega(dry season) during the past 30 years. Inconsistency trend shown in annual streamflow due to the variation exists in rainfall, temperature and land cover.

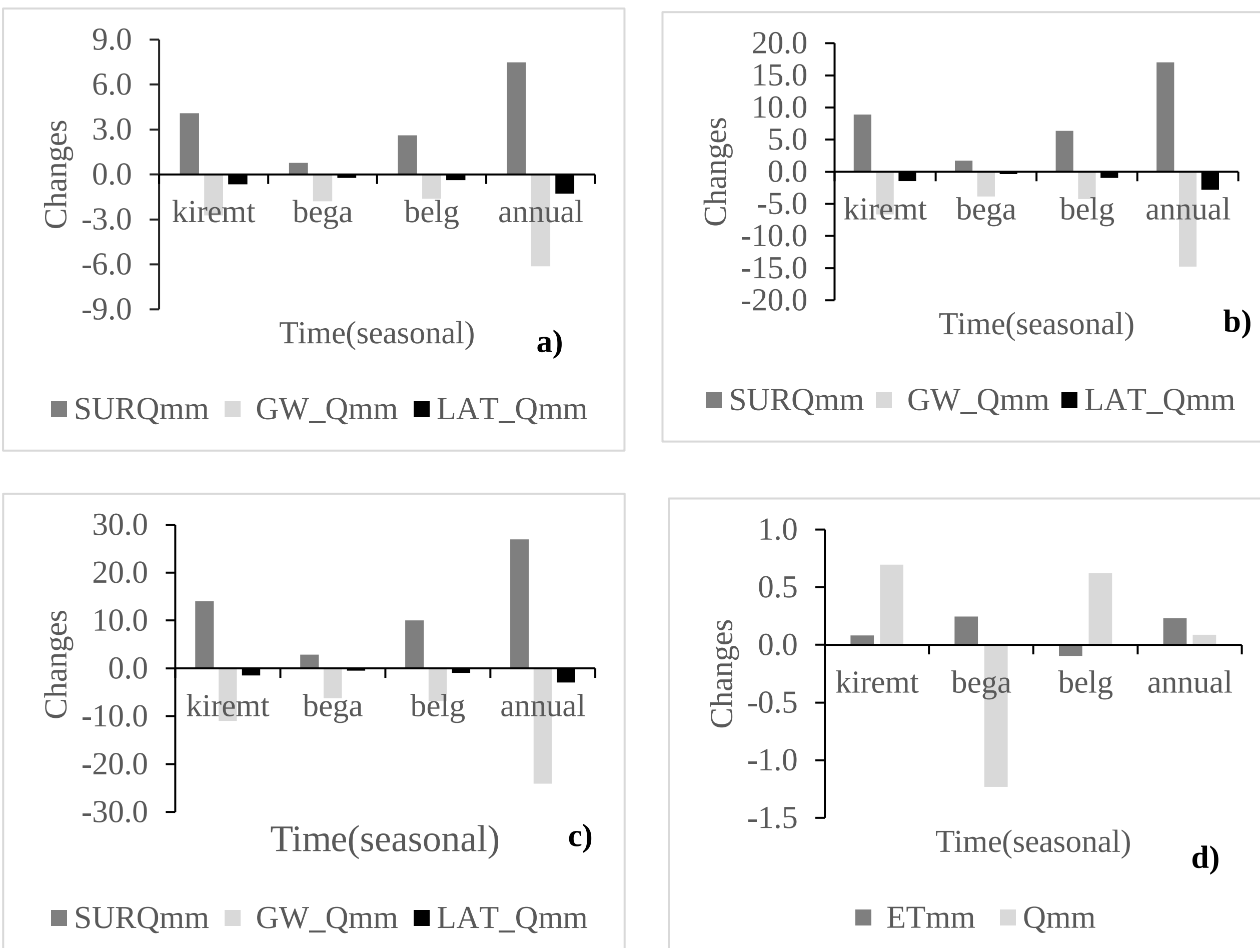

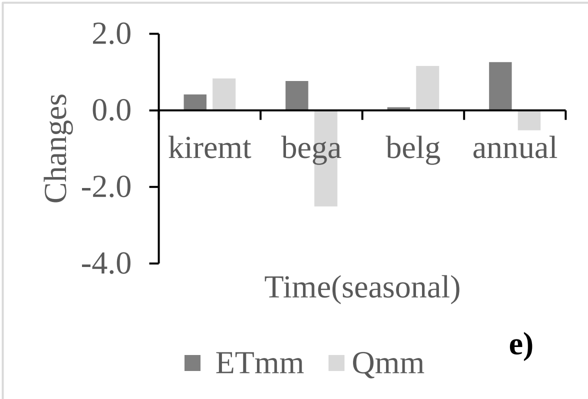

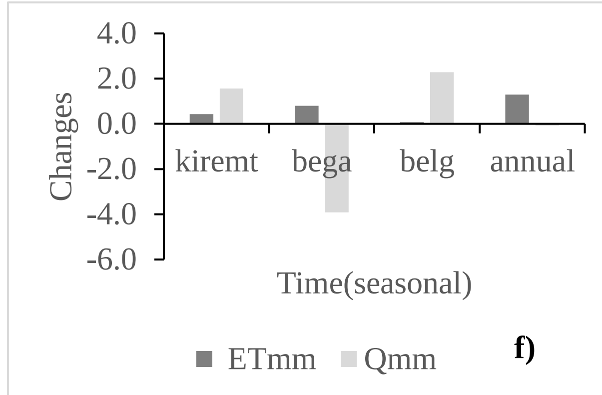

Figure 4.9 Changes of mean annual and seasonal contribution of surface runoff (SURQ), groundwater flow (QW_Q) and lateral flow (LAT_Q) as a),b),c) and evapotranspiration (ET), total streamflow (Q) as d),e),f) for baseline-altered period of (1989-2002,1989-2011,1989-2019)respectively.

5 SUMMARY AND CONCLUSION

5.1 Summary

Changes in land-use/land cover of Shaya Watershed in Genale-Dawa River Basin have been evaluated for understanding natural land and water resources protection. The image of land cover classes was conducted using ERDAS IMAGINE software under proposed the land map scenarios such as 1989, 2002, 2011, and 2019. The integrated remote sensing data were used to quantify LULC classification to apply the trend of changes between classes and could help to simulate water balance components. In this study, the Landsat 5TM, 7ETM, and 8OLI were downloaded from the USGS website for four land maps. Six dominant classes were classified as agriculture, forest, bareland, grassland, settlement, and shrublands using a supervised method of classification. The overall kappa statistics were 0.85, 0.94, 0.90 and 0.89 for land map 1989, 2002, 2011 and 2019 respectively. Therefore, the accuracy assessment was found to be in the range of acceptance criteria (i.e. > 0.8).

The result indicated that decreased trend was seen in forest, grassland, bareland, and shrubland by (10.64%, 9.88%, 2.15%, and 1.02%) in the period of (1989-2019) respectively. Whereas the increased trend was observed in agriculture and settlement classes by 17.97% and 5.71% in the same period.

Changes in LULC of Shaya Watershed has been assessed on water balance components using QSWAT modeling approaches. In this approach, spatial data (land, soil, slope) and non-spatial data (precipitation, temperature, relative humidity, wind speed and solar radiation) could help to simulate water balance variable like surface runoff yield, groundwater flow, lateral flow, evapotranspiration, and others. Therefore, the study was used to understand the impact of LULC changes on water resources for protection of environment

The sensitivity analysis and performance criteria of the model was applied based on monthly observed hydrograph before the output of QSWAT model had been analyzed. Accordingly, groundwater, soil, and watershed characteristics (ALPHA, CN, ESCO, GWQMN, SLSUBBSN, OV_N, etc.) were considered in this study. The calibration and validation of the model were determined for land map 2002 by SWAT-CUP under SUFI-2 optimization algorithm. The simulated and observed flow were fit as good performance at outlet of the watershed using NSE, R^2, and PBIAS values as objective functions.

The result from QSWAT revealed that surface runoff (Qs) was increased while groundwater flow (Qb) and lateral flow (Ql) were decreased in the last 30 years. A slight change was observed in evapotranspiration (ET) as increased and streamflow (Q) varied as up and down in wet and dry season in the watershed due to variation of precipitation distribution and land-use/land cover changes. The Qs/Q was increased from (26.4% to 30.7%), but Qb/Q and Ql/Q were decreased from (65% to 61.1%) and (8.7% to 8.2%) in the period of (1989-2019). In addition, the change of water balances was seen in seasonal patterns (e.g. Qs has increased by (14% &2.8%) in kiremt/wet and bega/dry season; while Qb has decreased by (11% & 6.3%) in the same season). To concluded that changes in LULC had potential to alter the water balances by rising surface runoff, decreasing groundwater recharge in the watershed. Therefore, these were required to monitor natural resources of land and water which are important aspects for the survival of life.

5.2 Conclusion

Water, Soil and Plants are important component of natural resources in the watershed that effectively preserved and utilized. But in recent time, they were under pressure due to population growth increases that overexploited and improper use of them. In this study, the finding shows that LULC changes play an important role in water balance indicated by increased surface runoff, river discharge fluctuated and decreased ground water flow due to rate of vegetation, grassland, shrubland were reduced and expansion of agriculture and settlement.

The following listed information are important recommended points under this study.

- There are insufficient gaged hydrometeorological recorded station data in the watershed. Such data affect the reliability of model output. Hence, to improve the gaged data continuously, it should be better if replacing automatic instrument instead of old.
- The result of QSWAT model indicated that surface runoff yield increased in the watershed. This result should have needed an action to control land-use/land cover

changes in the watershed. Therefore, it suggested to adopt the integrated water resource management to minimize the source of impact.

- It should be advisable to promote the land-use/land cover strategies, policies effectively in watershed communities to keep the security of water as safely.
- The study is mainly focused on the impact of land-use/land cover changes on water balances but not considered analysis of climate change, geology and another variable. So, it should be suggested for future researchers' if they are comprised such variable for better understanding water resource managements.

REFERENCE

Abbas, I. I., Muazu, K. M., & Ukoje, J. A. (2010). Mapping Land Use - land Cover and Change Detection in Kafur Local Government , Katsina , Nigeria (1995 - 2008) Using Remote Sensing and GIS. Research Journal of Environmental and Earth Sciences, 2(1), 6–12.

Abbaspour, K. C., Vaghefi, S. A., & Srinivasan, R. (2018). A Guideline for Successful Calibration and Uncertainty Analysis for Soil and Water Assessment : A Review of Papers from the 2016 International SWAT Conference. ii. https://doi.org/10.3390/w10010006

Addae, B., & Oppelt, N. (2019). Land-Use/Land-Cover Change Analysis and Urban Growth Modelling in the Greater Accra Metropolitan Area (GAMA), Ghana. Urban Science, 3(1), 26. https://doi.org/10.3390/urbansci3010026

Adeogun, A. G., Sule, B. F., Salami, A. W., & Daramola, M. O. (2014). Validation of SWAT Model for Prediction of Water Yield and Water Balance : Case Study of Upstream Catchment of Jebba Dam in Nigeria. International Journal of Physical, Nuclear Science and Engineering, 8(2), 1–7.

Aish, A. . (2014). Estimation of water balance components in the Gaza Strip with GIS based WetSpass model. Civil Environ Res, 6(11), 77–85.

Andualem, T. and Gebremariam, B. (2016). Impact of land use Land cover change on stream flow and sediment: A case study of Gilgel Abay Watershed, Lake Tana Sub-Basin,Ethiopia. International Journal of Technology Enhancements and Emerging Engineering Research, 3(1), 2347–4289.

Arnold, J. (2015). SWAT Model Use,Calibration and Validation. American Society of Agricultural and Biological Engineers, 55(4), 1491–1508.

Assefa, G. A. (2018). The impact of land use-land cover change on water availability in the Kulfo Watershed. Arbaminch University.

Ayele, G. T., Tebeje, A. K., Demissie, S. S., Belete, M. A., Jemberrie, M. A., Teshome, W. M., Mengistu, D. T., & Teshale, E. Z. (2018). Time series land cover mapping and change detection analysis using geographic information system and remote sensing, Northern Ethiopia. Air, Soil and Water Research, 11. https://doi.org/10.1177/1178622117751603

Baker, T. J., & Miller, S. N. (2013). Using the Soil and Water Assessment Tool (SWAT) to assess land use impact on water resources in an East African watershed. Journal of Hydrology, 486, 100–111. https://doi.org/10.1016/j.jhydrol.2013.01.041

Bansode, S., & Patil, K. (2016). Water Balance Assessment using Q-SWAT. International Journal of Engineering Research, ISSN(56), 2319–6890. https://doi.org/10.17950/ajar/v5s6/620

Butt, A., Shabbir, R., Ahmad, S. S., & Aziz, N. (2015). Land use change mapping and analysis using Remote Sensing and GIS: A case study of Simly watershed, Islamabad, Pakistan. Egyptian Journal of Remote Sensing and Space Science, 18(2), 251–259. https://doi.org/10.1016/j.ejrs.2015.07.003

Cunderlik, J. (2003). Hydrologic model selection for the CFCAS Project:Assessment of Water Resources Risk and Vulnerability to Changing Climatic Conditions.

Da Silva, M.G., de Aguiar Netto, A.D.O., de Jesus Neves, R.J., Do Vasco, A.N., Almeida, C. and Faccioli, G. G. (2015). Sensitivity analysis and calibration of hydrological modeling of the watershed Northeast Brazil. Journal of Environmental Protection, 6(08), 837.

Devia, G. K., Ganasri, B. P., & Dwarakish, G. S. (2015). A Review on Hydrological Models. Aquatic Procedia, 4(December), 1001–1007. https://doi.org/10.1016/j.aqpro.2015.02.126

Dile, Y., Srinivasan, R., & George, C. (2019). QGIS Interface for SWAT (QSWAT) version 1.8. July, 98. https://swat.tamu.edu/media/116301/qswat-manual_v18.pdf

Fang, G., Yuan, Y., Gao, Y., Huang, X., & Guo, Y. (2018). Assessing the effects of urbanization on flood events with urban agglomeration polders type of flood control pattern using the HEC-HMS model in the Qinhuai River Basin, China. Water (Switzerland), 10(8). https://doi.org/10.3390/w10081003

Gashaw, T., Tulu, T., Argaw, M., & Worqlul, A. W. (2018). Modeling the hydrological impacts of land use/land cover changes in the Andassa watershed, Blue Nile Basin, Ethiopia. Science of the Total Environment, 619–620, 1394–1408. https://doi.org/10.1016/j.scitotenv.2017.11.191

Getachew, T. (2013). Lake Tana Reservoir Water Balance Model. International of Journal of Application or Innovation In Engineering and Management(IJAIEM), 2(3), 2219–4847.

Getahun, Y. S., & HAJ, V. L. (2015). Assessing the Impacts of Land Use-Cover Change on

Hydrology of Melka Kuntrie Subbasin in Ethiopia, Using a Conceptual Hydrological Model. Journal of Waste Water Treatment & Analysis, 06(03). https://doi.org/10.4172/2157-7587.1000210

Githui, F., Mutua, F., & Bauwens, W. (2009). Estimating the impacts of land-cover change on runoff using the soil and water assessment tool (SWAT): Case study of Nzoia catchment, Kenya. Hydrological Sciences Journal, 54(5), 899–908. https://doi.org/10.1623/hysj.54.5.899

Gumindoga, W., Rientjes, T., Haile, A., & Dube, T. (2014). Predicting stream flow for land cover changes in the Upper Gilgel Abay River Basin, Ethiopia: A TOPMODEL based approach. Physics and Chemistry of the Earth, 76, 3–15.

Hamad, R., Balzter, H., & Kolo, K. (2018). Predicting land use/land cover changes using a CA-Markov model under two different scenarios. Sustainability (Switzerland), 10(10), 1–23. https://doi.org/10.3390/su10103421

Holder, A. J., Rowe, R., McNamara, N. P., Donnison, I. S., & McCalmont, J. P. (2019). Soil & Water Assessment Tool (SWAT) simulated hydrological impacts of land use change from temperate grassland to energy crops: A case study in western UK. GCB Bioenergy, 11(11), 1298–1317. https://doi.org/10.1111/gcbb.12628

Jemberie, M., & Gebremariam, B. (2016). Novateur Publications International Journal of Innovations in Engineering Research and Technology [Ijiert] Evaluation of Land Use Land Cover Change on Stream Flow: a Case Study Ofdedissa Sub Basin, Abay Basin, South Western Ethiopia. 3(8), 44–60.

Kamali, B., Abbaspour, K. C., & Yang, H. (2017). Assessing the Uncertainty of Multiple Input Datasets in the Prediction of Water Resource Components. https://doi.org/10.3390/w9090709

Kashinde, P. L., & Patil, K. A. (2017). Water Balance Study Of Watershed (Gv-53) Using Qswat In Aurangabad District. 6, 38–45.

Kassa, T., & Forech, G. (2009). Watershed Hydrological Responses to Changes in Land Use and Land Cover , and Management Practices at Hare Watershed , Ethiopia. Ph.D Thesis, University of Siegen, Germany, 229.

Kassahun, N. and Mohamed, M. (2018). Groundwater Potential Assessment and Characterization of Genale-Dawa River Basin. Open Journal of Modern Hydrology, 8(4), 126–144.

Kindu, M., Schneider, T., Teketay, D., & Knoke, T. (2013). Land use/land cover change analysis using object-based classification approach in Munessa-Shashemene landscape of the ethiopian highlands. Remote Sensing, 5(5), 2411–2435. https://doi.org/10.3390/rs5052411

Kleidon, A., Renner, M., Porada, P., & Biogeochemie, M. (2014). Estimates of the climatological land surface energy and water balance derived from maximum convective power. 2201–2218. https://doi.org/10.5194/hess-18-2201-2014

Li, Z., Liu, H., Zhao, W., Yang, Q., Yang, R., & Liu, J. (2019). Estimation of Evapotranspiration and Other Soil Water Budget Components in an Irrigated Agricultural Field of a Desert Oasis, Using Soil Moisture Measurements. Hydrology and Earth System Sciences Discussions, October, 1–22. https://doi.org/10.5194/hess-2019-89

Lillesand, T.M., Kiefer, R.W. and Chipman, J. . (2008). Digital image interpretation and analysis. Remote sensing and image interpretation. 6, 545–581.

Lyu, L., Wang, X., Sun, C., Ren, T., & Zheng, D. (2019). Quantifying the effect of land use change and climate variability on greenwater resources in the Xihe River Basin, Northeast China. Sustainability (Switzerland), 11(2). https://doi.org/10.3390/su11020338

Marhaento, H. (2018). Attribution of changes in the water balance of a tropical catchment to land use change using the SWAT model’. Effects of changes in land use and climate on water availability of a tropical catchment. 13–26. https://doi.org/https://doi.org/10.3990/1.9789036544917.

Marhaento, Hero, Booij, M. J., Rientjes, T. H., & Hoekstra, A. Y. (2017). Attribution of changes in the water balance of a tropical catchment to land use change using the SWAT model. Hydrological Processes, 31(11), 2029–2040. https://doi.org/10.1002/hyp.11167

Myburgh, G. and Van Niekerk, A. (2014). Impact of training set size on object-based land cover classification: A comparison of three classifiers. . . International Journal of Applied Geospatial Research (IJAGR), 5(3), 49–67.

Näschen, K., Diekkrüger, B., Evers, M., Höllermann, B., Steinbach, S., & Thonfeld, F. (2019).

The Impact of Land Use/Land Cover Change (LULCC) on Water Resources in a Tropical Catchment in Tanzania under Different Climate Change Scenarios. Sustainability (Switzerland), 11(24). https://doi.org/10.3390/su11247083

Neitsch, S. ., Arnold, J. ., Kiniry, J. ., & Williams, J. . (2011). Soil & Water Assessment Tool Theoretical Documentation Version 2009. Texas Water Resources Institute, 1–647. https://doi.org/10.1016/j.scitotenv.2015.11.063

Nugroho, P., Marsono, D., Sudira, P., & Suryatmojo, H. (2013). The 3 rd International Conference on Sustainable Future for Human Security Impact of land-use changes on water balance. Procedia Environmental Sciences, 17, 256–262. https://doi.org/10.1016/j.proenv.2013.02.036

Owuor, S. O., Butterbach-Bahl, K., Guzha, A. C., Rufino, M. C., Pelster, D. E., Díaz-Pinés, E., & Breuer, L. (2016). Groundwater recharge rates and surface runoff response to land use and land cover changes in semi-arid environments. Ecological Processes, 5(1). https://doi.org/10.1186/s13717-016-0060-6

Palmate, S. S., Wagner, P. D., Pandey, A., & Fohrer, N. (2018). Effects of land use change on the water resources of the Basoda basin using the SWAT model. 1, 1–17.

Premanand, B. D., Satishkumar, U., Babu, B. M., & Parasappa, S. K. (2018). QSWAT Model Calibration and Uncertainty Analysis for Stream Flow Simulation in the Patapur Micro-Watershed Using Sequential Uncertainty Fitting Method (SUFI-2). 7(04), 831–852.

Raja, R., Anand, V., Kumar, A., Maithanis,S., and Kumar, V. (2013). Wavelet based post classification change detection technique for urban growth monitoring. Journal of the Indian Society of Remote Sensing, 41(1), 35–43. http://doi.org/10.1007/s12524-011-0199-7.

Rientjes, T. H. M., Haile, A. T., Kebede, E., Mannaerts, C. M. M., Habib, E., & Steenhuis, T. S. (2011). Changes in land cover, rainfall and stream flow in Upper Gilgel Abbay catchment, Blue Nile basin - Ethiopia. Hydrology and Earth System Sciences, 15(6), 1979–1989. https://doi.org/10.5194/hess-15-1979-2011

Santillan, J., Makinano, M., & Paringit, E. (2011). Integrated landsat image analysis and hydrologic modeling to detect impacts of 25-year land-cover change on surface runoff in a

Philippine watershed. Remote Sensing, 3(6), 1067–1087. https://doi.org/10.3390/rs3061067

Serur, A. B., & Sarma, A. K. (2016). Evaluation of the ArcSWAT Model in Simulating Catchment Hydrology : In Weyib River Basin , Bale Mountainous Area of Southeastern Ethiopia. International Journal of Innovative and Emerging Research in Engineering, 3(2).

Setegn, S., Fidaqu, Y., and Mal, B. (2009). Impact of Landuse/Land Cover Transformations on Alemeya Lake, Ethiopia. Journal of Indian Water Resources Society, 29, 40–45.

Shao, G., Guan, Y., Zhang, D., Yu, B., & Zhu, J. (2018). The impacts of climate variability and land use change on streamflow in the Hailiutu River Basin. Water (Switzerland), 10(6). https://doi.org/10.3390/w10060814

Shimelis Gebriye Setegn , Fikadu Yohannes , Shoeb Quraishi, V. M. C. and B. C. M. (2009). Impact of Land Use / Land Cover Transformations on Alemaya Lake, Ethiopia. Journal of Indian Water Resources Society, 29(3), 40–45.

Srinivasan, R., & George, C. (2015). QGIS Interface for SWAT (QSWAT) October 2015. Setup for Robit Watershed, Lake Tana Basin, October, 20–21. https://doi.org/10.13140/RG.2.1.1060.7201

Tegegne, G., Hailu, D., & Aranganathan, P. S. M. (2013). Lake Tana Reservoir Water Balance Model. International Journal of Application or Innovation in Engineering & Management (IJAIEM), 2(3), 474–478. www.ijaiem.org

Tesfahun, A. M.,& Dereje ,T., M. (2019). Modeling change of Land use on Hydrological Response of River by Remedial Measures using Arc SWAT: Case of Weib Catchment, Ethiopia. International Journal of Innovative Technology and Exploring Engineering (IJITEE), 8(11), 2278–3075. https://doi.org/10.35940/ijitee.J9531.0981119

Tesfalem, A. and Behailu, N. (2018). Impact of Land Use Land Cover Dynamics on Water Balance, Lake Ziway Watershed, Ethiopia. Hydrology: Current Research, 9(4), 309.

Thakkar, A., Dessai, V., Patel, A.and Potdra, M. (2015). Landuse/Land cover classification using remote sensing data and derived indices in a heterogeneous landscape of a khan-kali watershed,Gujarat. Asian Journal of Geoinformatics, 14(4).

Tibebe, D. & Bewket, W. (2011). Surface runoff and soil erosion estimation using the SWAT model in the Keleta watershed, Ethiopia. Land Degradation & Development, 22(6), 551–564.

Tomer, M & Schilling, K. (2009). A simple approach to distinguish land-use and climate-change effects on watershed hydrology. Journal of Hydrology, 376(1–2), 24–33.

Tufa, D. F., Abbulu, Y. and Srinivasa Rao, G. V. R. (2015). Hydrological Impacts due to Land-Use and Land-Cover Changes of Ketar Watershed, Lake Ziway Catchment, Ethiopia. International Journal of Civil Engineering and Technology, 6(10), 36–45.

Welde, K., & Gebremariam, B. (2017). Effect of land use land cover dynamics on hydrological response of watershed: Case study of Tekeze Dam watershed, northern Ethiopia. In International Soil and Water Conservation Research (Vol. 5, Issue 1). Elsevier B.V. https://doi.org/10.1016/j.iswcr.2017.03.002

World Bank Group. (2015). East Asia’s changing urban landscape: Measuring a decade of spatial growth. World Bank Publications.

Yadav, Y., Bahadur, B., Chhetri, K., Raymajhi, S., Rajtiwari, K., & Kumar, B. (2019). Dynamics of Land use Land Cover Change and Mapping of Tree Outside Forest (TOF) in Terai , Nepal. 19(1), 4–9. https://doi.org/10.19080/IJESNR.2019.18.556002

Yalcin, A. (2008). GIS-based landslide susceptibility mapping using analytical hierarchy process and bivariate statistics in Aedesen, Turkey.

Yesuf, H. M., Assen, M., Melesse, A. M., & Alamirew, T. (2015). Detecting land use/land cover changes in the Lake Hayq (Ethiopia) drainage basin, 1957-2007. Lakes and Reservoirs: Research and Management, 20(1), 1–18. https://doi.org/10.1111/lre.12082

ANNEX

Annex A: Accuracy assessment Result

Table A.1 Output of accuracy assessment for LULC classification map of 1989 year

	Reference Data							Users	Commission
Classified Data	1	2	3	4	5	6	Total	Accuracy	Error
Settlement (1)	12	1	0	0	0	1	14	83.33%	16.67%
Bareland (2)	0	6	0	0	0	1	7	60.00%	40.00%
Forest (3)	0	0	158	0	4	0	162	94.61%	5.39%
Shrubland (4)	0	0	4	48	5	0	57	84.00%	16.00%
Grassland (5)	0	0	3	0	60	1	64	84.51%	15.49%
Agriculture (6)	0	5	0	0	0	71	76	88.75%	11.25%
Total	12	14	165	48	69	74	382		
Producers Accuracy	83.33%	42.86%	95.76%	87.50%	86.96%	95.95%			
Omission Error	16.67%	57.14%	4.24%	12.50%	13.04%	4.05%			

Overall Classification Accuracy = 89.00%
Overall Kappa Statistics = 0.8496

Table A.2 Output of accuracy assessment for LULC classification map of 2002 year

	Reference Data							Users	Commission
Classified Data	1	2	3	4	5	6	Total	Accuracy	Error
Settlement (1)	18	0	0	0	1	1	20	90.00%	10.0%
Bareland (2)	0	11	0	1	0	0	12	78.57%	21.4%
Forest (3)	0	0	132	2	0	0	134	97.78%	2.2%
Shrubland (4)	0	0	2	57	0	0	59	96.61%	3.4%
Grassland (5)	0	0	1	1	56	0	58	93.33%	6.7%
Agriculture (6)	0	0	1	0	1	99	101	97.06%	2.9%
Total	18	11	136	61	58	100	384		
Producers Accuracy	100.00%	100.00%	97.06%	93.44%	96.55%	99.00%			
Omission Error	0.00%	0.00%	2.94%	6.56%	3.45%	1.00%			

Overall Classification Accuracy = 95.65%
Overall Kappa Statistics = 0.9431

Table A.3 Output of accuracy assessment for LULC classification map of 2011 year

	Reference Data							Users	Commission
Classified Data	1	2	3	4	5	6	Total	Accuracy	Error
Settlement (1)	25	0	0	0	4	1	30	83.33%	16.67%
Bareland (2)	0	4	0	0	0	0	4	100.00%	0.00%
Forest (3)	2	0	122	2	2	4	132	91.73%	8.27%
Shrubland (4)	0	1	1	36	0	0	38	94.74%	5.26%
Grassland (5)	1	0	2	0	55	0	58	91.67%	8.33%
Agriculture (6)	0	1	1	0	0	120	122	96.00%	4.00%
Total	28	6	126	38	61	125	384		
Producers Accuracy	89.29%	66.67%	96.83%	94.74%	90.16%	96.00%			
Omission Error	10.71%	33.33%	3.17%	5.26%	9.84%	4.00%			

Overall Classification Accuracy = 92.84%

Overall Kappa Statistics = 0.9044

Table A.4: Output of accuracy assessment for LULC classification map of 2019 year

	Reference Data							Users	Commission
Classified Data	1	2	3	4	5	6	Total	Accuracy	Error
Settlement (1)	39	0	2	0	2	0	43	88.64%	11.36%
Bareland (2)	1	6	0	0	0	3	10	60.00%	40.00%
Forest (3)	0	0	98	3	1	0	102	96.08%	3.92%
Shrubland (4)	0	0	2	52	3	0	57	89.66%	10.34%
Grassland (5)	0	0	2	1	39	3	45	82.98%	17.02%
Agriculture (6)	1	1	1	0	1	122	126	94.57%	5.43%
Total	41	7	105	56	46	128	383		
Producers Accuracy	95.12%	85.71%	93.33%	92.86%	84.78%	95.31%			
Omission Error	4.88%	14.29%	6.67%	7.14%	15.22%	4.69%			

Overall Classification Accuracy = 91.30%

Overall Kappa Statistics = 0.8877

Annex B: Hydro-metrological data in Shaya Watershed

Table B.1 Areal mean annual metrological data (1989-2018)

year	Precipitation(mm)	Tmax(°c)	Tmin(°c)	Wind(m/s)	Solar (MJ/m2)	Humidity (%)
1989	1773.2	19.3	5.4	1.8	7.4	70.2
1990	1477.2	19.9	5.4	1.5	7.5	66.9
1991	1134.4	20.3	5.3	1.9	7.4	63.7
1992	1771.3	19.5	5.6	1.9	6.9	67.4
1993	1478.0	20.0	5.6	1.9	7.3	65.8
1994	1452.5	19.8	5.8	1.9	7.2	64.0
1995	1176.2	19.4	5.8	1.8	7.3	66.6
1996	1092.7	19.0	5.5	1.7	7.1	66.5
1997	1286.6	19.4	6.0	1.7	7.1	66.2
1998	1231.4	19.5	6.5	1.5	7.2	68.5
1999	968.7	19.3	5.6	1.5	7.9	65.2
2000	935.4	19.6	5.7	1.4	8.0	61.8
2001	1082.6	19.5	6.0	1.5	7.7	66.6
2002	816.8	19.6	6.7	1.4	7.5	73.7
2003	905.6	19.5	6.6	1.3	7.8	65.5
2004	931.0	19.9	6.4	1.4	7.8	66.4
2005	919.1	19.7	6.6	1.4	8.0	65.4
2006	1213.9	19.4	7.0	1.4	7.0	70.9
2007	1071.4	19.4	6.7	1.4	7.4	68.0
2008	962.9	19.5	6.5	1.4	7.6	65.1
2009	977.3	19.7	6.9	1.4	7.2	65.2
2010	1046.6	19.4	7.2	1.4	6.7	70.6
2011	725.5	19.9	6.5	1.4	7.5	65.4
2012	865.7	19.9	6.2	1.4	7.2	63.9
2013	1064.9	19.8	6.7	0.8	6.7	66.7
2014	859.5	22.3	9.4	1.5	6.9	64.7
2015	702.9	23.4	8.4	1.5	7.6	65.2
2016	772.9	19.7	6.9	1.5	8.2	71.7
2017	940.3	20.3	7.3	1.3	7.6	71.1
2018	861.0	20.4	7.7	1.5	6.6	68.0
Grand Total	1083.3	19.9	6.5	1.5	7.4	66.9

Table B.2 Mean monthly precipitation(mm) for four station

Month	Goba	Rira	Robe	Dinsho	Stream flow(m/s)
Jan	23.2	32.8	13.7	15.5	1.5
Feb	18.0	15.4	18.4	23.0	1.4
Mar	59.7	69.4	61.1	65.0	1.6
Apr	134.5	101.1	106.4	139.3	4.5
May	89.2	90.7	91.7	102.3	4.3
Jun	56.7	36.8	59.2	51.7	2.4
Jul	98.4	101.0	97.5	158.6	6.7
Aug	139.4	110.9	143.9	159.4	12.8
Sep	142.2	63.0	109.9	119.9	8
Oct	120.6	108.5	81.8	115.9	12.9

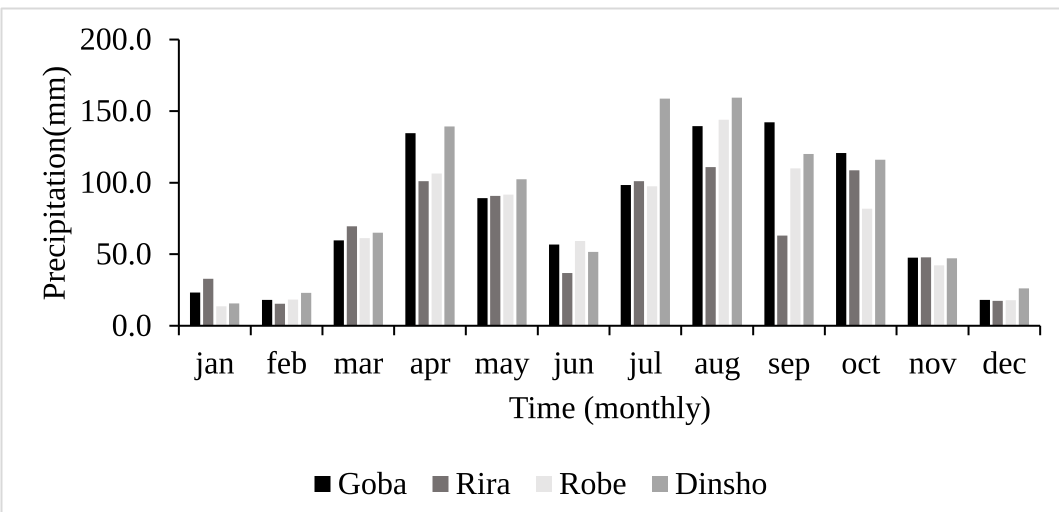

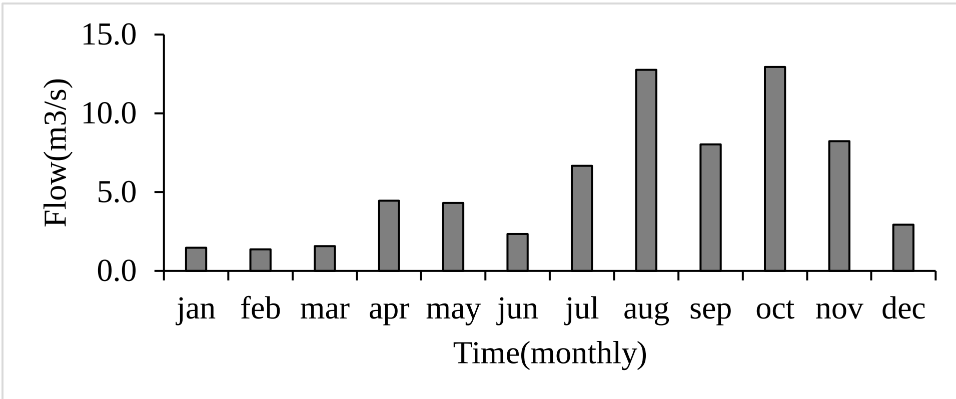

Figure B.2 Mean monthly observed flow(1989-2014)

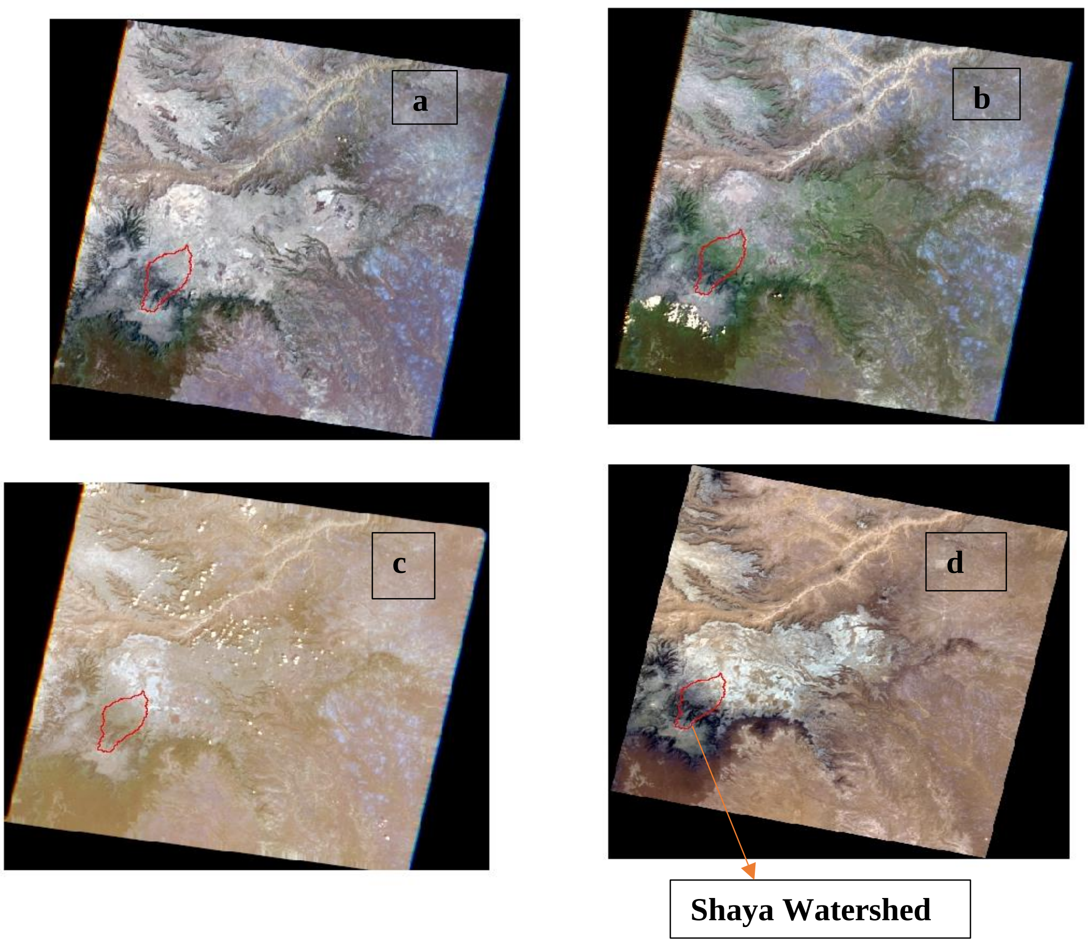

Figure B.3 Landsat image a), b), c) and d) for (1989, 2002, 2011 and 2019) land classification that have been used for LULC analysis